Q

BRL

REPORT NO. 1180

NOVEMBER 1962

DETERMINATION OF VISCOELASTIC MODEL
CONSTANTS FROM DYNAMIC MECHANICAL
PROPERTIES OF LINEAR VISCOELASTIC MATERIALS

W. Goldberg
N. W. Dean

BALLISTIC RESEARCH LABORATORIES

ABERDEEN PROVING GROUND, MARYLAND

ASTIA AVAILABILITY NOTICE

Qualified requestors may obtain copies of this report from ASTIA.

BALLISTIC RESEARCH LABORATORIES

REPORT NO. 1180

NOVEMBER 1962

DETERMINATION OF VISCOELASTIC MODEL CONSTANTS FROM DYNAMIC MECHANICAL PROPERTIES OF LINEAR VISCOELASTIC MATERIALS

W. Goldberg
N. W. Dean

Interior Ballistics Laboratory

ABERDEEN PROVING GROUND, MARYLAND

BALLISTIC RESEARCH LABORATORIES

REPORT NO. 1180

WGoldberg/NWDean/bj
Aberdeen Proving Ground, Md.
November 1962

DETERMINATION OF VISCOELASTIC MODEL CONSTANTS FROM DYNAMIC MECHANICAL PROPERTIES OF LINEAR VISCOELASTIC MATERIALS

ABSTRACT

A semi-analytical method of determining the generalized Voigt model which represents the dynamic mechanical properties of a linear viscoelastic material over a range of frequencies of three decades is presented. This model representation is shown to be equivalent to the differential operator formulation of the linear viscoelastic stress-strain law. The method is applied to complex creep compliance data for N.B.S. polyisobutylene at 22 different temperatures. In general, the compliances calculated from the models differ from the experimental data by less than 5%.

A summary of spring-dashpot model theory is presented in Appendix A. The equivalence of the differential operator stress-strain relation and the generalized Voigt model is demonstrated in Appendix B.

Page intentionally blank

Page intentionally blank

Page intentionally blank

TABLE OF CONTENTS

Page intentionally blank

Page intentionally blank

Page intentionally blank

INTRODUCTION

A number of commonly used materials such as plastics, rubbers, fibers, etc. exhibit viscoelastic properties such as creep and relaxation. A case in point is the solid propellant rocket fuel where elastic analyses are inadequate for relatively long time conditions, such as slump during storage, and for extremely short-time dynamic conditions, such as impact and sudden acceleration. Problems such as these are currently being solved using techniques of the theory of linear viscoelasticity.[1], [2]* However, the application of these techniques is dependent upon the formulation of the linear viscoelastic stress-strain laws from experimental data in such a manner as to represent the mechanical properties of the actual material.

Presented in this report is a semi-analytical method of determining the generalized Voigt model which will accurately represent the dynamic mechanical properties of a linear viscoelastic substance over a range of frequencies of three decades.[3] This model representation is equivalent to the differential operator formulation of the linear viscoelastic stress-strain laws.

The method employed is based upon the analogy between linear electrical networks and spring-dashpot mechanical systems.[4], [5] A transfer function is constructed to represent the generalized Voigt model. The asymptotic approximation method originally devised by Baum is used in conjunction with a least squares computer program to determine the viscoelastic model constants from dynamic creep compliance data. This method can be applied to viscoelastic materials exhibiting a wide range of dynamic mechanical behavior and represents a significant improvement over previous model fitting techniques.[3]

LINEAR ISOTHERMAL VISCOELASTIC STRESS-STRAIN RELATIONS

In the theory of linear isothermal viscoelasticity, a viscoelastic solid is specified by the existence of a relation connecting stress, σ, and strain, ϵ:

$$P\left[\sigma\right] = Q\left[\epsilon\right] \tag{1}$$

---

* Superscripts indicate references at the end of this paper.

7

where P and Q are linear differential operators with respect to time. Thus,

$$P = p_0 + p_1 \frac{d}{dt} + p_2 \frac{d^2}{dt^2} + \dots + p_r \frac{d^r}{dt^r} \qquad (2)$$

$$Q = q_0 + q_1 \frac{d}{dt} + q_2 \frac{d^2}{dt^2} + \dots + q_m \frac{d^m}{dt^m} \qquad (3)$$

The p's and q's are constants which represent the mechanical properties of the material at a given temperature. These constants cannot be measured directly, but must be calculated from experimental data in which both the stress and strain are known as functions of time. Although the stress-strain, $\sigma - \epsilon$, relations for a linearly viscoelastic material may also be represented by hereditary integrals, [1], [2], [5] it has been found that the determination of the stresses in a viscoelastic body subjected to transient loading is considerably simplified if Eqs. (1), (2) and (3) are used to specify the material behavior.

MODEL REPRESENTATION

The expression $P\left[\sigma\right] = Q\left[\epsilon\right]$ is often visualized as a mathematical representation of a mechanical model, consisting of a network of springs and dashpots. A summary of the theory of spring-dashpot models is presented in Appendix A. The model used to describe the mechanical properties of materials in this report is the generalized Voigt model.
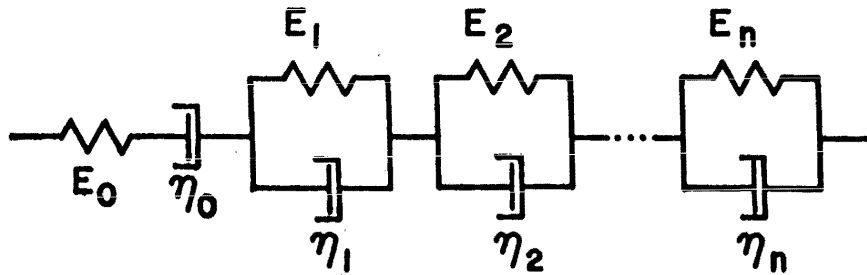

FIG. I. THE GENERALIZED VOIGT MODEL

This model exhibits both instantaneous elasticity and long-term creep and is mathematically better suited to describe experimental dynamic creep data than is the generalized Maxwell model. The operational form of the stress-strain, $\sigma - \epsilon$ relation, for this model is then given by

$$\epsilon(t) = \frac{\sigma(t)}{E_0} + \left[\frac{1}{\eta_0 \frac{d}{dt}} + \sum_{i=1}^{n} \frac{1}{E_i + \eta_i \frac{d}{dt}} \right] \sigma(t) \tag{4}$$

COMPLEX CREEP COMPLIANCE

The steady state response of this model to a sinusoidal stress is given by

$$J^*(\omega) = \frac{\epsilon}{\sigma} = J'(\omega) - iJ''(\omega) \tag{5}$$

where the time dependence of both ϵ and σ is of the form $e^{i\omega t}$. This ratio, J^*, is known as the complex compliance with J' and J'' called the storage and loss compliances respectively. The non-zero imaginary function, $J''(\omega)$, implies a phase difference between the oscillations of stress and strain. Both J' and J'' are functions of ω which can be measured experimentally over the frequency range of interest. Substitution of steady state sinusoidal variation in Eq. (4), which means replacement of the operator $\frac{d}{dt}$ with $i\omega$, and comparing with Eq. (5) yields

$$J^*(\omega) = \frac{1}{E_0} + \frac{1}{\eta_0 i\omega} + \sum_{j=1}^{n} \frac{1}{E_j + i\omega\eta_j} \tag{6}$$

and therefore

$$J'(\omega) = \frac{1}{E_0} + \frac{E_1}{E_1^2 + \eta_1^2 \omega^2} + \cdots + \frac{E_n}{E_n^2 + \eta_n^2 \omega^2} \tag{7}$$

$$= \frac{1}{E_0} + \sum_{j=1}^{n} \frac{E_j}{E_j^2 + \omega^2 \eta_j^2}$$

9

$$J''(\omega) = \frac{1}{\eta_0\omega} + \frac{\eta_1\omega}{E_1^2 + \eta_1^2\omega^2} + \cdots + \frac{\eta_n\omega}{E_n^2 + \eta_n^2\omega^2} \tag{8}$$

$$= \frac{1}{\eta_0\omega} + \sum_{j=1}^{n} \frac{\eta_j\omega}{E_j^2 + \eta_j^2\omega^2}$$

The complex compliance may also be written as the ratio of two polynomials. In Eqs. (2) and (3), let $r = m$; this corresponds to a viscoelastic material exhibiting instantaneous elasticity. Then choose $p_0 = 1$ and $q_0 = 0$; this allows for the presence of an isolated dashpot which permits long term viscous flow.

Then if $\sigma = e^{i\omega t}$

$$\epsilon = J^*(\omega)e^{i\omega t} \tag{9}$$

and from (2) and (3) we have

$$P\left[\sigma\right] = \left[1 + p_1 i\omega + p_2(i\omega)^2 + \cdots + p_m(i\omega)^m\right]e^{i\omega t} \tag{10}$$

and

$$Q\left[\epsilon\right] = J^*(i\omega)\left[q_1 i\omega + q_2(i\omega)^2 + \cdots + q_m(i\omega)^m\right]e^{i\omega t} \tag{11}$$

but

$$P\left[\sigma\right] = Q\left[\epsilon\right]$$

Therefore

$$J^*(i\omega) = \frac{1 + p_1 i\omega + p_2(i\omega)^2 + \cdots + p_m(i\omega)^m}{q_1 i\omega + q_2(i\omega)^2 + \cdots + q_m(i\omega)^m} \tag{12}$$

Now let $i\omega = s$. Then

$$H(s) = \frac{p(s)}{q(s)} = \frac{1 + p_1 s + p_2 s^2 + \cdots + p_m s^m}{q_1 s + q_2 s^2 + \cdots + q_m s^m} \tag{13}$$

Cauer,[7] Alfrey, Gross and others have shown the analogy between electrical networks and mechanical models. From this analogy, $H(s)$ is defined as the system transfer function, and exhibits the same properties as the transfer function for an RC network. The equivalence of the differential operator $\sigma - \epsilon$ representation and the generalized Voigt model is presented in

Appendix B along with a discussion of the properties of the system transfer function $H(s)$. Another convenient form of the transfer function $H(s)$ can be derived by letting λ_1, λ_2, λ_3, $\ldots$ λ_{m-1} be the roots of the equation

$$q_1 + q_2 s + q_3 s^2 + \ldots + q_m s^{m-1} = 0 \tag{14}$$

and letting μ_1, μ_2, $\ldots$, μ_m be the roots of the equation

$$1 + p_1 s + p_2 s^2 + \ldots + p_m s^m = 0 \tag{15}$$

The properties of $H(s)$, as found in Appendix B, require that the μ_i and λ_i be negative real constants. Then $H(s)$ may be written in the form

$$H(s) = J^*(s) = \frac{k(s - \mu_1)(s - \mu_2) \ldots (s - \mu_m)}{s(s - \lambda_1)(s - \lambda_2) \ldots (s - \lambda_{m-1})} \tag{16}$$

where k is a positive real constant. This form of $H(s)$ is useful in calculating $p(s)$ and $q(s)$ once the λ_i and μ_i have been determined.

DETERMINATION OF MODEL CONSTANTS FROM DYNAMIC CREEP COMPLIANCE DATA

Having shown that the generalized Voigt model is equivalent to the differential operator description of viscoelastic material behavior, the appropriate values of η_j and E_j are required to fit experimental data. The dynamic creep compliance data consists of values of J' and J'' at different values of ω. From the relations

$$\left| J^* \right| = \sqrt{(J')^2 + (J'')^2} \tag{17}$$

and

$$\phi = \tan^{-1} \frac{J''}{J'}$$

the values of $\left| J^* \right|$, the absolute value of the complex compliance, and ϕ, the phase angle, are calculated.

The graphical, semi-analytical method reported by Welch,[8] and originally applied to circuit synthesis is then used to determine the approximate location of the poles of the transfer function, $H(s)$. This method consists of (1) construction of a graph of ϕ versus $\log \omega$ and (2) construction of a graph of $\log \left| J^* \right|$ vs $\log \omega$ from the experimental data.

Careful study of the phase angle plot, along with some knowledge of the effect of various spacings of poles and zeros on the phase angle as a function of frequency, results in an initial placement of the poles and zeros.[9] The possible location of these poles and zeros is then verified on the graph $|J*|$ vs ω. These poles are located at $s = \lambda_j$ in the complex s plane. These values of λ_j are then substituted into Eqs. (7) and (8) along with the relation

$$\lambda_j = -E_j/n_j \quad \text{(Appendix B) to yield} \tag{18}$$

$$J'(\omega) = \frac{1}{E_0} - \frac{\lambda_1/\eta_1}{\lambda_1^2 + \omega^2} - \frac{\lambda_2/\eta_2}{\lambda_2^2 + \omega^2} - \cdots\cdots - \frac{\lambda_n/\eta_n}{\lambda_n^2 + \omega^2}$$

$$\tag{19}$$

$$J''(\omega) = \frac{1}{\eta_0\omega} + \frac{\omega/\eta_1}{\lambda_1^2 + \omega^2} + \frac{\omega/\eta_2}{\lambda_2^2 + \omega^2} + \cdots\cdots + \frac{\omega/\eta_n}{\lambda_n^2 + \omega^2}$$

Now let $\dfrac{1}{E_0} = A;\quad \dfrac{1}{\eta_0} = B;\qquad \dfrac{1}{\eta_j} = C_j$ $\tag{20}$

Then Eq. (15) becomes

$$J'(\omega) = A - \frac{\lambda_1 C_1}{\lambda_1^2 + \omega^2} - \cdots\cdots - \frac{\lambda_n C_n}{\lambda_n^2 + \omega^2}$$

$$\tag{21}$$

$$J''(\omega) = \frac{B}{\omega} + \frac{\omega C_1}{\lambda_1^2 + \omega^2} + \cdots\cdots + \frac{\omega C_n}{\lambda_n^2 + \omega^2}$$

Eqs. (21) are then solved for the values of A, B, and C_j using experimental data for J' and J'' at from 8 to 16 different values of ω. The solution of this overdetermined system is obtained using a least squares program on the BRL ORDVAC digital computer. This program applies Legendre's principle, as outlined in Reference 10, to solve the normal equations derived from the overdetermined system of linear equations. The computer uses the values of λ_j and calculates positive A, B, and C_j along with the values of J' and J'' at the different values of ω for comparison with the input data. Since the relative experimental error is generally constant, the least squares program minimizes the relative error in the fitting procedure.[11]*

* This procedure has proven more effective than the method employed in Reference 11.

Study of these results provides indications as to possible motion of the poles and zeros of H(s) to improve the data fit. For example, if the first choice of the poles λ_j is in error, the constants C_j, as calculated by least squares, are negative. These negative C_j do not correspond to a spring dashpot model. Possible error in only one $\lambda_j = \lambda_k$ results in only C_k being negative, thus providing a clue to the source of the trouble. Once the A, B, and C_j are known, the values of E_j and η_j can be determined from Eqs. (18) and (20). The problem of generating p(s) and q(s) from the E_j and η_j is most easily approached through the equivalence of two forms of H(s). Let $i\omega = s$ in Eq. (6) and substitute Eq. (20) to get

$$J^*(s) = H(s) = A + \frac{B}{s} + \sum_{j=1}^{n} \frac{C_j}{s - \lambda_j} \qquad (22)$$

Equating Eqs. (22) and (16), we find

$$k = A = \frac{1}{E_0}$$

and the μ_i are the roots of the equation,

$$A + \frac{B}{s} + \sum_{j=1}^{n} \frac{C_j}{s - \lambda_j} = 0. \qquad (23)$$

Solution of Eq. (23) using the BRL ORDVAC digital computer by means of successive subdivision of the intervals between λ_j and λ_{j+1}, provides the values of the μ_i.

APPLICATION OF PROCEDURE TO N.B.S. POLYISOBUTYLENE

Published data for N.B.S. polyisobutylene,[12] Table No. I, are used to provide an example of the application of this procedure. The data for 22 different temperatures are fitted, since this represents a wide range of viscoelastic behavior. The results of these calculations are tabulated in Tables No. II and No. III and are illustrated in Figures 10 thru 18. Figures 2 thru 9 show the graphs of ϕ vs log ω and $|J^*|$ vs log ω for four characteristic temperatures: -40.4°C, -29.8°C, -9.9°C, and +50.0°C. These ϕ vs log ω graphs indicate considerably different viscoelastic behavior, and therefore the location of the λ_j, as well as their spacing, requires some knowledge of pole and zero interaction.

TABLE I SUMMARY OF DYNAMIC MECHANICAL DATA ON POLYISOBUTYLENE *

T °C	Frequency cps	30	40	45	60	72	80	100	140	200	210	280	400	600	800	1000	1400	1500	2000	2800	3000	4000	4200	5100
−44.6	J' cm²/dyne(×10⁻⁹)	...		...	...		...	...	...		...	0.151	0.145	0.136	0.123	0.132		0.119	0.111		0.108			0.0995
	J'' cm²/dyne(×10⁻⁹)				0.345		0.244	0.200			0.166	0.142	0.118	0.0955	0.0831	0.0697		0.0551	0.0506		0.0368			0.0309
−40.4	J' cm²/dyne(×10⁻⁹)	...		...	0.617		0.490	0.411			0.308	0.264	0.212	0.186	0.163	0.167		0.149	0.137		0.129			0.112
	J'' cm²/dyne(×10⁻⁹)			0.823							0.336	0.264	0.230	0.177	0.151	0.129		0.107	0.0921		0.0651			0.0601
−34.7	J' cm²/dyne(×10⁻⁹)	2.20		1.59	1.17			0.958	0.805		0.660	0.566	0.467	0.367	0.304	0.268		0.214	0.182		0.130			0.107
	J'' cm²/dyne(×10⁻⁹)							0.848	0.702		0.571	0.478	0.387	0.308	0.254	0.248		0.216	0.188		0.165			0.139
−29.8	J' cm²/dyne(×10⁻⁹)	3.96		2.92	2.07			1.70	1.43		1.13	1.02	0.796	0.639	0.553	0.486		0.415	0.336		0.248		0.226	0.219
	J'' cm²/dyne(×10⁻⁹)							1.41	1.19		0.997	0.852	0.656	0.512	0.440	0.398		0.368	0.278		0.220			0.153
−25.0	J' cm²/dyne(×10⁻⁹)	6.79		4.98	3.66			2.97	2.39		1.80	1.58	1.26	1.02	0.880	0.777		0.622	0.558		0.421		0.350	
	J'' cm²/dyne(×10⁻⁹)				2.54			2.17	1.81		1.48	1.25	1.01	0.825	0.703	0.625		0.526	0.422		0.329		0.302	
−19.9	J' cm²/dyne(×10⁻⁹)	6.59		5.23	3.93			3.42	2.63		2.25	1.88	1.52	1.24	1.03	0.947		0.792	0.646		0.526		0.388	
	J'' cm²/dyne(×10⁻⁹)	11.8		8.91		6.56		5.38	4.20		3.14	2.63	2.06	1.63	1.37	1.23		0.977	0.893		0.687		0.634	
−14.8	J' cm²/dyne(×10⁻⁹)	11.5		8.96	7.48		6.17	5.55	4.51	3.64		2.99	2.38	1.85		1.47			0.949	0.752				
	J'' cm²/dyne(×10⁻⁹)	20.1		14.8	12.2		10.2	8.76	6.93	5.47		4.42	3.49	2.65		1.91			1.40	1.10				
−9.9	J' cm²/dyne(×10⁻⁹)	19.7		14.8	12.0		10.0	8.70	7.06	5.87		4.71	3.55	2.78	2.43	2.18		1.62	1.25	1.08		1.05		
	J'' cm²/dyne(×10⁻⁹)	31.1		22.5	18.8		15.8	13.7	11.0	8.54		6.81	5.55	4.19	3.44	2.94		2.29	2.19	1.58		1.64		
−5.0	J' cm²/dyne(×10⁻⁹)	29.8		23.0	19.2		16.2	13.7	11.0	8.71		6.89	5.35	4.09	3.40	2.90			1.61	1.42				
	J'' cm²/dyne(×10⁻⁹)	40.4		32.7	27.9		23.2	20.4	16.3	12.9		10.4	8.39	6.21	5.15	4.43			3.02	2.06				
−0.10	J' cm²/dyne(×10⁻⁹)	50.4		37.2	30.1		25.0	21.2	16.8	13.1		10.4	7.88	5.77	4.98	4.37		3.24						
	J'' cm²/dyne(×10⁻⁹)	55.9		45.5	39.0		33.6	29.2	24.0	19.2		15.6	12.4	9.04	7.72	6.75		5.53						
4.9	J' cm²/dyne(×10⁻⁹)	75.7		56.3	46.2		37.8	32.1	26.0	20.1		15.9	12.2	8.87	7.52	6.12		4.67						
	J'' cm²/dyne(×10⁻⁹)	72.8		61.2	53.5		46.4	40.9	33.9	27.5		23.0	17.9	13.6	11.4	10.3		8.13						
9.8	J' cm²/dyne(×10⁻⁹)	106.		80.2	66.2		54.6	47.2	37.5	29.0		23.1	16.8	12.7	10.4	9.02		6.68	5.13	3.84				3.26
	J'' cm²/dyne(×10⁻⁹)	86.8		76.1	67.9		60.6	53.8	46.0	37.9		31.8	25.4	20.0	17.2	15.5		10.5	10.2	7.33				5.86
14.8	J' cm²/dyne(×10⁻⁹)	140.		110.	92.7		77.2	66.4	53.1	42.1		33.4	24.9	17.6	15.7	13.2	9.52		7.72	6.06				5.00
	J'' cm²/dyne(×10⁻⁹)	96.4		88.1	81.9		74.8	71.6	61.3	49.6		41.0	33.0	26.3	23.6	20.9	15.4		14.3	10.9				8.21
19.8	J' cm²/dyne(×10⁻⁹)	176.		144.	124.		106.	89.5	71.0	57.1		46.9	35.7	26.1	21.8	18.8			10.9	8.92				7.04
	J'' cm²/dyne(×10⁻⁹)	99.4		96.8	93.2		87.4	84.8	75.1	64.8		51.9	44.3	35.8	29.8	27.2			19.4	14.8				11.7
25.0	J' cm²/dyne(×10⁻⁹)	204.	184.	182.	156.		137.	119.	96.4	79.0		65.3	51.2	38.5	32.1	27.1	20.7		15.7	12.1				8.94
	J'' cm²/dyne(×10⁻⁹)	102	93.6	107.	98.0		97.8	95.2	88.1	77.9		65.0	56.4	46.9	41.0	36.4	30.1		26.3	20.5				16.6
30.2	J' cm²/dyne(×10⁻⁹)				198.			154.	129.	109.		90.0	70.3	53.8	46.2	38.4			22.9	19.1				
	J'' cm²/dyne(×10⁻⁹)				103.			103.	98.6	84.2		79.6	70.8	61.2	51.4	47.6			35.5	26.8				
34.9	J' cm²/dyne(×10⁻⁹)				227.		204.	187.	168.	142.		116.	92.1	73.7	59.7	51.9	44.2			26.3				
	J'' cm²/dyne(×10⁻⁹)				102.		99.0	102.	96.8	97.8		90.7	81.2	72.1	61.0	58.3	43.5			31.4				
40.0	J' cm²/dyne(×10⁻⁹)			271.	252.		231.	217.	190.	167.		146.	117.	95.0	78.5	70.2	55.6							
	J'' cm²/dyne(×10⁻⁹)			76.7	89.0		94.0	94.3	93.0	94.1		97.4	94.3	81.1	73.7	69.2	52.7							
50.0	J' cm²/dyne(×10⁻⁹)			307.	266.		278.	260.	251.	225.		199.	177.	141.	123.	113.	89.8							
	J'' cm²/dyne(×10⁻⁹)			55.7	64.2		79.2	81.9	91.2	92.1		95.2	101.	93.0	90.3	78.1	74.7							
59.8	J' cm²/dyne(×10⁻⁹)			294.	295.		292.	282.	269.	260.		239.	221.	188.										
	J'' cm²/dyne(×10⁻⁹)			40.2	51.0		53.5	58.4	67.6	71.0		82.1	91.8	96.3										
80.0	J' cm²/dyne(×10⁻⁹)			310.	319.		315.		302.	290.		282.	277.	257.										
	J'' cm²/dyne(×10⁻⁹)			32.3	34.9		26.8		40.2	43.5		50.0	60.3	71.3										
99.9	J' cm²/dyne(×10⁻⁹)			302.				316.	314.	310.		293.	295.	285.										
	J'' cm²/dyne(×10⁻⁹)			23.4				28.3	29.2	31.1		31.7	33.8	40.2	47.1									

* REF. 12 – TABLE 2

74

TABLE II. SUMMARY OF CALCULATED DYNAMIC MECHANICAL DATA ON POLYISOBUTYLENE

T°C	FREQUENCY CPS / ω RADIANS/SEC.	30 / 188.50	40 / 251.33	45 / 282.74	60 / 376.99	72 / 452.39	80 / 502.66	100 / 628.32	140 / 879.65	200 / 1256.6	210 / 1319.5	280 / 1759.3	400 / 2513.3	600 / 3769.9	800 / 5026.6	1000 / 6283.2	1400 / 8796.5	1500 / 9424.8	2000 / 12566.	2800 / 17593.	3000 / 18850.	4000 / 25133.	4200 / 26389.	5100 / 32044.
-44.6	J' CM²/DYNE (x 10⁻⁹)											.154	.150	.142	.134	.128		.116	.110		.104			.0979
	J'' "											.152	.116	.0910	.0783	.0698		.0558	.0471		.0376			.0310
-40.4	J' "										.300	.263	.227	.193	.174	.162		.146	.136		.125			.109
	J'' "										.348	.289	.230	.178	.148	.128		.0990	.0842		.0700			.0590
-34.7	J' "							.832	.711		.580	.493	.397	.313	.271	.248		.211	.191		.164			.132
	J'' "							.982	.815		.863	.573	.470	.364	.301	.259		.200	.170		.137			.103
-29.8	J' "							1.39	1.21		.980	.827	.666	.527	.452	.404		.329	.283		.223			.154
	J'' "							1.68	1.42		1.16	1.00	.823	.647	.545	.479		.385	.333		.274			.209
-25.0	J' "					2.52		2.16	1.80		1.45	1.25	1.04	.845	.722	.636		.506	.432		.345		.281	
	J'' "					3.56		2.95	2.42		1.89	1.58	1.28	1.02	.875	.774		.615	.523		.419		.349	
-19.9	J' "	6.41		5.28		4.05		3.38	2.78		2.18	1.84	1.51	1.23	1.08	.968		.786	.668		.510		.386	
	J'' "	11.5		8.87		6.52		5.25	4.23		3.27	2.70	2.13	1.63	1.38	1.22		.986	.859		.716		.609	
-14.8	J' "	11.5		8.89	7.47		6.27	5.46	4.44	3.58		2.94	2.40	1.94		1.49			.948	.741				
	J'' "	19.7		14.9	12.2		10.1	8.75	7.00	5.52		4.42	3.50	2.69		1.99			1.35	1.07				
-9.9	J' "	20.0		14.5	11.9		9.97	8.70	7.08	5.64		4.52	3.59	2.81	2.39	2.11		1.65	1.36	1.06	1.01			
	J'' "	30.2		22.9	18.8		15.5	13.4	10.8	8.69		7.02	5.55	4.24	3.52	3.07		2.42	2.04	1.83	1.55			
-5.0	J' "	29.6		23.4	19.1		15.6	13.3	10.7	8.53		6.81	5.28	3.98	3.28	2.83			1.74	1.40				
	J'' "	39.1		32.1	27.5		23.2	20.1	16.3	13.1		10.7	8.53	6.53	5.39	4.65			2.88	2.21				
-0.10	J' "	49.9		37.4	30.5		24.8	21.1	16.3	12.6		9.98	7.91	6.06	5.00	4.31		3.27						
	J'' "	54.5		45.1	38.9		33.4	29.6	24.2	19.3		15.5	12.3	9.56	7.96	6.89		5.31						
4.9	J' "	74.9		56.6	45.8		37.2	31.9	25.3	19.8		15.6	12.0	9.02	7.40	6.32		4.67						
	J'' "	76.1		61.4	53.6		46.5	41.0	34.0	27.6		22.6	18.4	14.3	11.9	10.3		7.59						
9.8	J' "	104.		80.7	66.1		54.3	46.8	37.5	29.2		22.7	17.3	12.9	10.5	8.94		6.59	5.26	4.03		3.07		
	J'' "	84.9		77.0	68.8		60.4	54.2	46.0	38.4		32.1	26.0	20.2	16.9	14.7		11.3	9.37	7.39		5.62		
14.8	J' "	139.		111.	93.2		77.7	66.9	52.9	41.2		32.5	25.1	18.7	15.3	13.0	10.3		7.93	6.14		4.66		
	J'' "	96.5		89.4	82.5		75.2	69.2	59.8	50.2		42.1	34.6	27.3	23.0	20.0	16.2		13.0	10.4		8.02		
19.9	J' "	171.		145.	125.		105.	91.3	73.0	57.0		45.1	35.5	27.1	22.3	19.1			11.6	8.89		6.65		
	J'' "	97.8		97.9	94.9		89.3	83.7	74.2	63.6		53.8	44.4	35.7	30.5	26.9			17.8	14.5		11.4		
25.0	J' "	203.	186.	178.	159.		138.	122.0	99.3	79.3		64.4	51.4	38.9	31.7	27.1	21.3		16.2	12.1		8.64		
	J'' "	100.	100.	100.	99.6		97.7	94.5	86.7	76.0		66.2	56.9	47.3	40.6	36.3	30.3		25.0	20.5		16.1		
30.2	J' "				197.			156.	131.	108.		89.0	71.4	55.2	45.6	39.1			23.6	18.3				
	J'' "				104.			102.	95.9	88.0		79.7	70.1	59.4	52.4	47.2			33.0	27.4				
34.9	J' "				220.		204.	189.	166.	140.		115.	93.9	74.3	62.3	53.7	42.1			26.1				
	J'' "				99.4		100.	101.	101.	98.2		91.3	81.4	70.1	62.9	57.4	48.7			30.2				
40.0	J' "		276.		253.		233.	217.	194.	170.		147.	122.	95.5	78.9	67.9	54.4							
	J'' "		77.7		88.4		93.6	95.6	96.3	95.5		93.9	90.1	81.7	73.2	65.7	53.6							
50.0	J' "		310.		295.		283.	271.	250.	224.		199.	174.	145.	125.	109.	88.9							
	J'' "		56.0		68.2		74.4	81.1	90.0	95.5		96.6	95.5	92.7	88.5	83.0	71.3							
59.8	J' "		310.		299.		290.	282.	269.	254.		237.	216.	189.										
	J'' "		41.1		48.4		54.0	58.7	65.8	73.5		81.4	89.9	97.6										
80.0	J' "		325.		317.		311.		299.	293.		285.	275.	257.										
	J'' "		32.3		35.1		36.6		39.8	43.9		50.3	59.6	71.6										
95.5	J' "		331.				317.	315.	307.	301.		296.	288.	276.										
	J'' "		23.5				28.7	29.2	29.9	31.5		34.7	39.8	46.3										

15

TABLE III

Model Constants

$T°C$	A	B	C_1	C_2	C_3	C_4	C_5	$-\lambda_1$	$-\lambda_2$	$-\lambda_3$	$-\lambda_4$	$-\lambda_5$
	$\frac{cm^2}{dyne}$ (x 10^{-9})	$\frac{cm^2}{dyne\ sec}$ (x 10^{-9})			$\frac{cm^2}{dyne\ sec}$ (x 10^{-9})					rad/sec		
-44.6	.05519	237.7	.5395	349.2	4487.			3800	6000	100000		
-40.4	.06347	213.7	243.7	329.3	156.1	2877.		650	3300	11500	45000	
-34.7	.08636	282.3	288.4	779.1	80.34	334.3	2689.	300	1700	3700	7700	27000
-29.8	.05545	683.2	570.6	913.6	534.6	1367.	5204.	730	1690	4600	10800	30000
-25.0	.1130	1091.	1134.	607.0	2530.	1157.	6928.	555	1650	4800	14200	30000
-19.9	.07215	1620.	1297.	2204.	3572.	14710		240	1150	6400	25600	
-14.8	.4062	1535.	2133.	2283.	3200.	12810		76	480	1750	10000	
-9.9	.5033	979.3	5000.	2268.	5319.	3055.	18470	76	480	1340	3800	12500
-5.0	.8822	4379.	7151.	1287.	10910	19260		240	580	1750	9000	
-0.1	1.078	2399.	9457.	12070	15690	31290		120	600	3000	12000	
+4.9	1.843	3844.	16800	11480	18790	43580		185	790	1950	8400	
+9.8	1.629	4091.	23010	9168.	30640	40070	53370	200	760	1450	6100	17000
+14.8	2.336	1939.	19930	33730	43220	37770	97970	145	570	2100	6000	17000
+19.8	2.978	5664.	36290	53280	85110	160700		290	1000	4400	17500	
+25.0	3.365	4756.	13110	71380	122600	264500		165	610	3000	15000	
+30.2	3.654	4744.	58810	113000	200500	396000		400	1600	6000	25600	
+34.9	17.56	11470	26250	144600	32720	374300		400	1240	3280	7350	
+40.0	31.78	3220.	51460	29960	236600	268300		450	1100	12600	6600	
+50.0	52.34	910.8	8843.	135700	12420	664300		220	1100	3000	5600	
+59.8	10.93	168.0	6630.	39800	293400	1913000		200	800	3200	12800	
+80.0	102.0	1860.	16030	13290	808500	1544000		400	1600	6400	25600	
+99.9	205.7	236.5	16250	6804.	592400			400	1600	6400		

FIG. 2-PHASE ANGLE ϕ FOR POLYISOBUTYLENE
AT (T = - 40.4 °C)
vs. ω
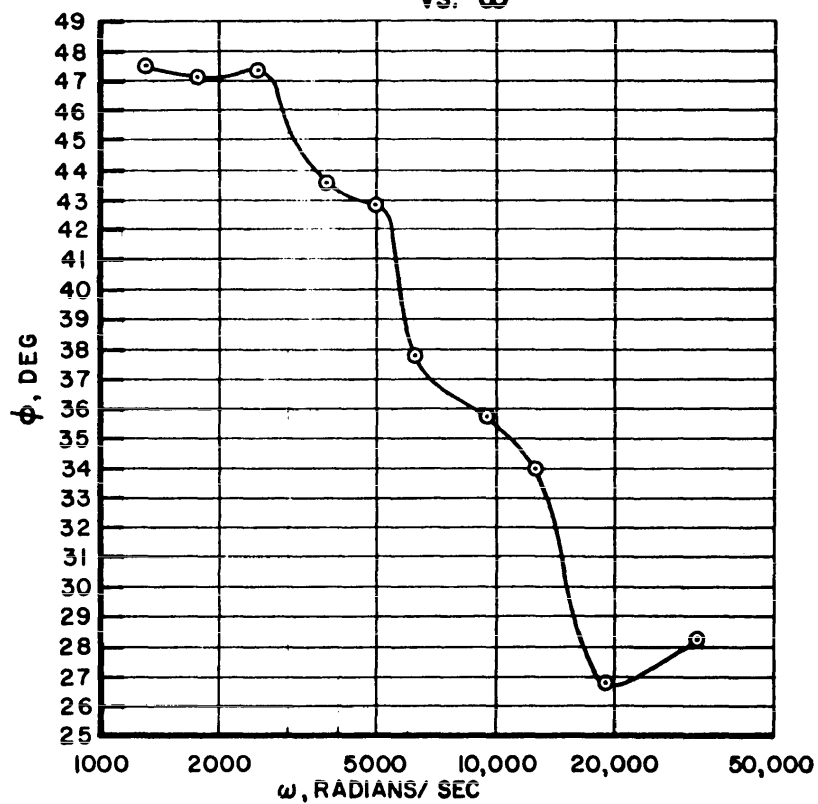
ϕ, DEG

ω, RADIANS/ SEC

FIG. 3-SHEAR COMPLIANCE $|J^*|$ FOR POLYISOBUTYLENE
AT (T = - 40.4° C)
vs. ω
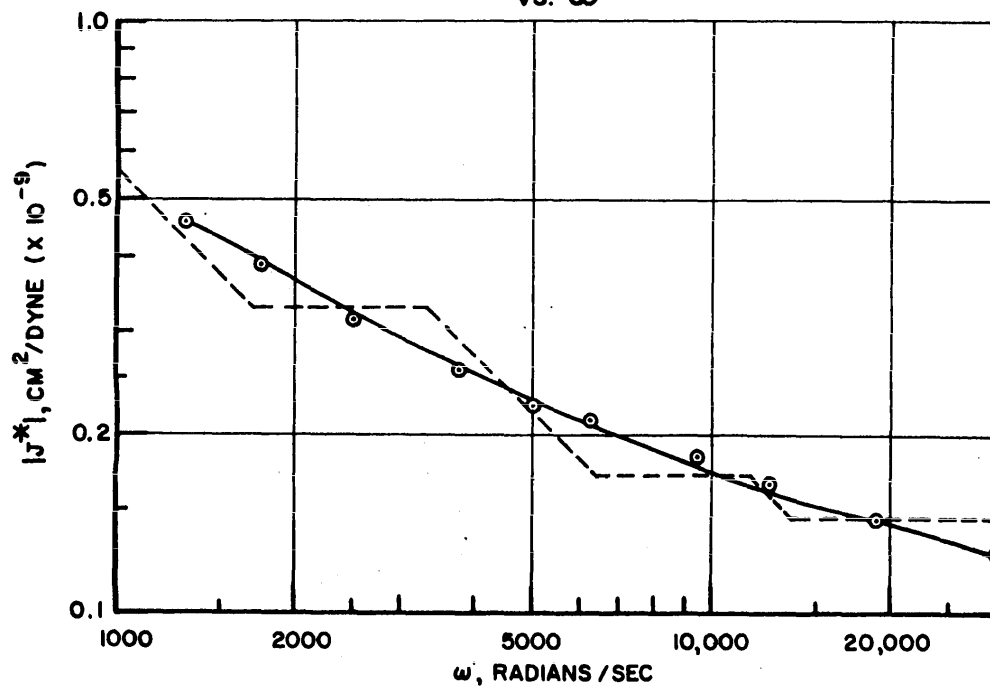
$|J^*|$, CM^2/DYNE (x 10^{-9})

ω, RADIANS /SEC

FIG. 4-PHASE ANGLE ϕ FOR POLYISOBUTYLENE
AT (T = − 29.8° C)
vs. ω

FIG. 5 − SHEAR COMPLIANCE $|J^*|$ FOR POLYISOBUTYLENE
AT (T = − 29.8°C)
vs. ω

FIG.6- PHASE ANGLE ϕ FOR POLYISOBUTYLENE
AT (T = - 9.9°C)
vs. ω

FIG. 7 - SHEAR COMPLIANCE $|J^*|$ FOR POLYISOBUTYLENE
AT (T = - 9.9°C)
VS. ω

19
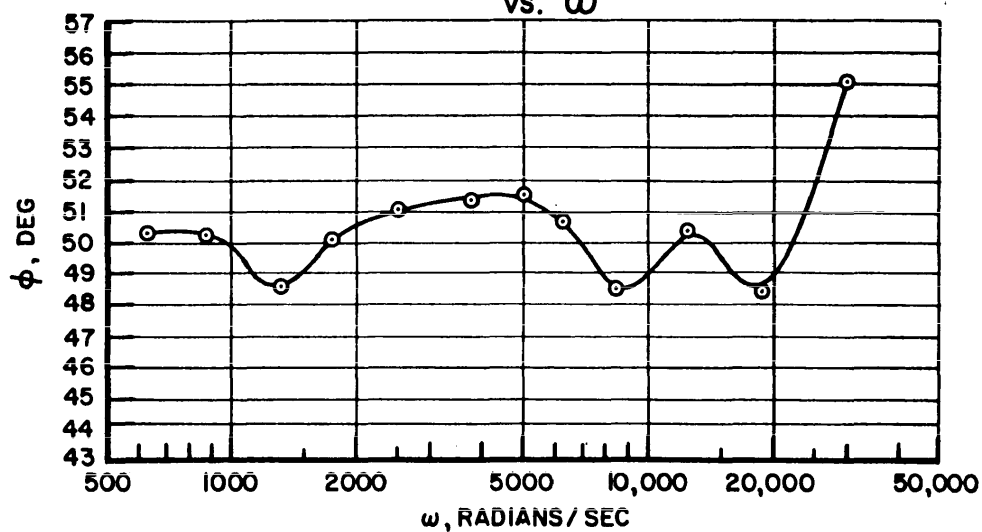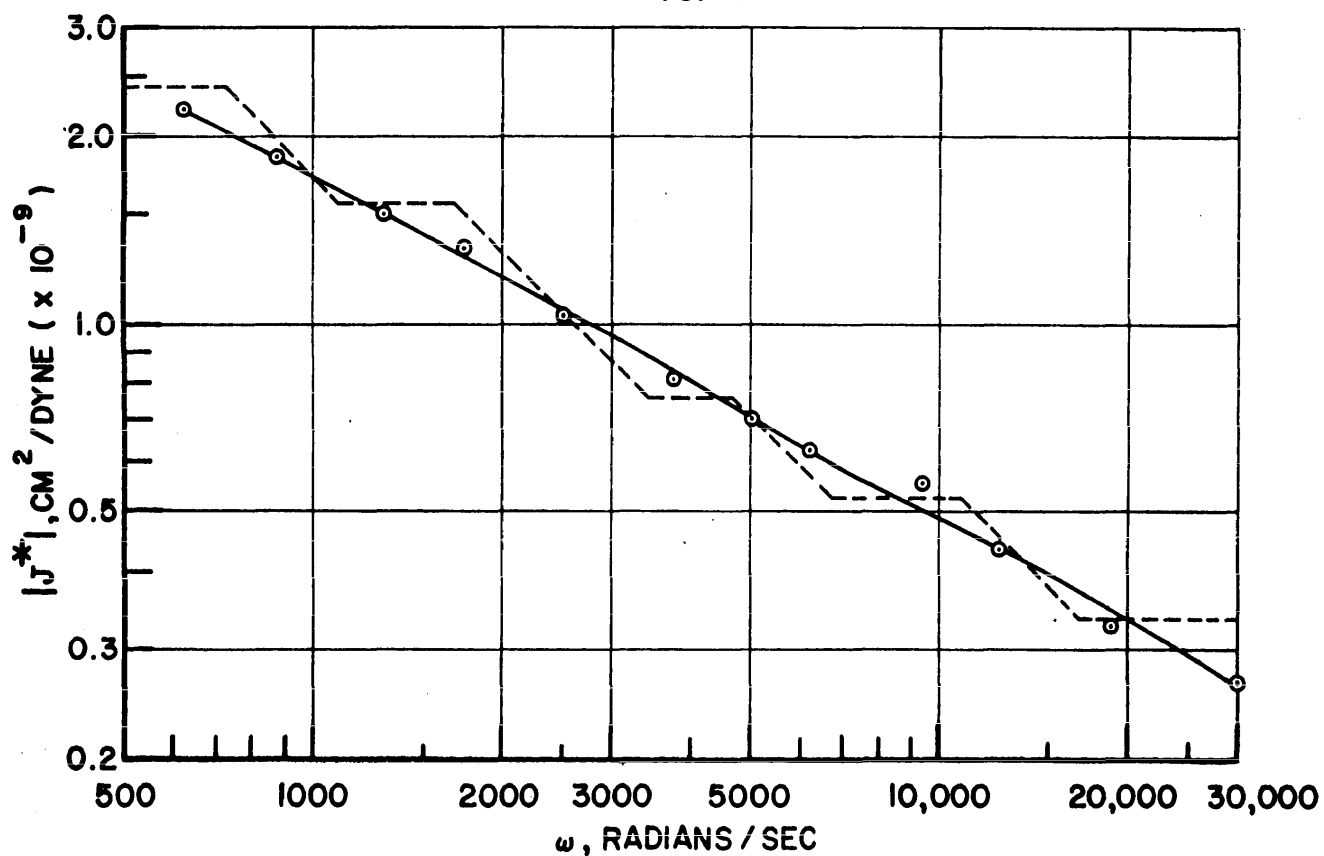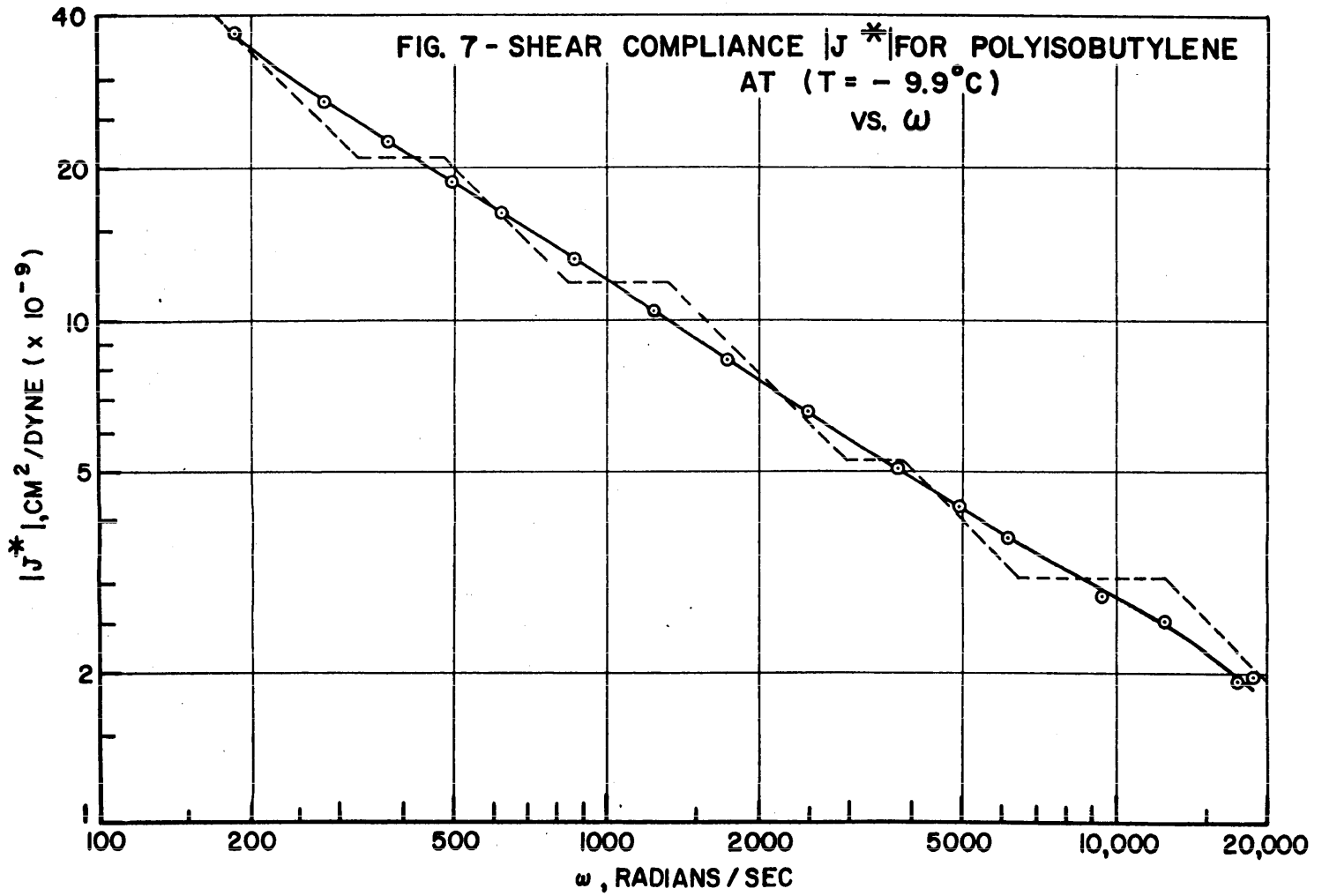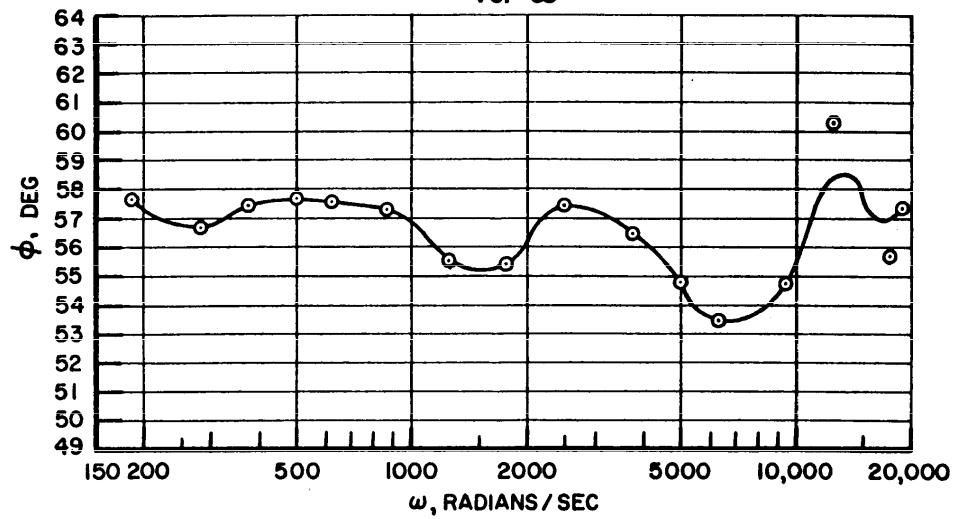
FIG. 8 — PHASE ANGLE ϕ FOR POLYISOBUTYLENE AT (T = 50.0° C) vs. ω
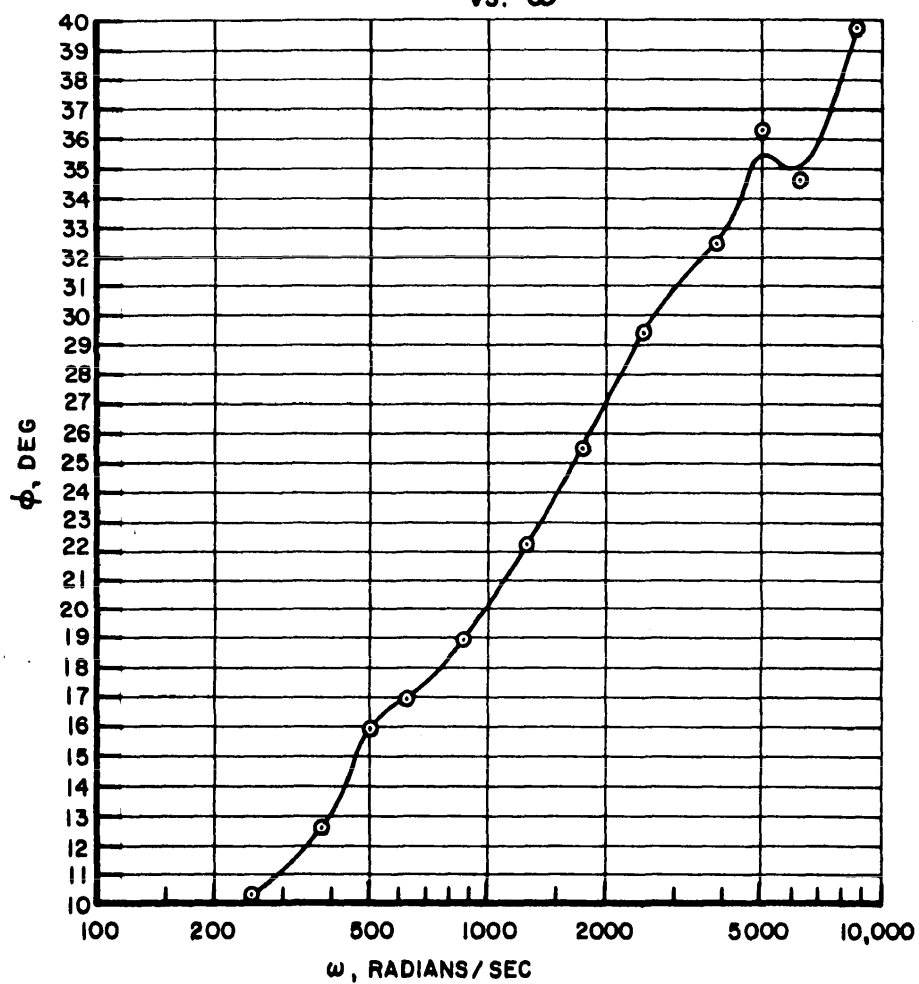
FIG. 9 - SHEAR COMPLIANCE $|J^*|$ FOR POLYISOBUTYLENE AT (T = + 50.0° C) vs. ω
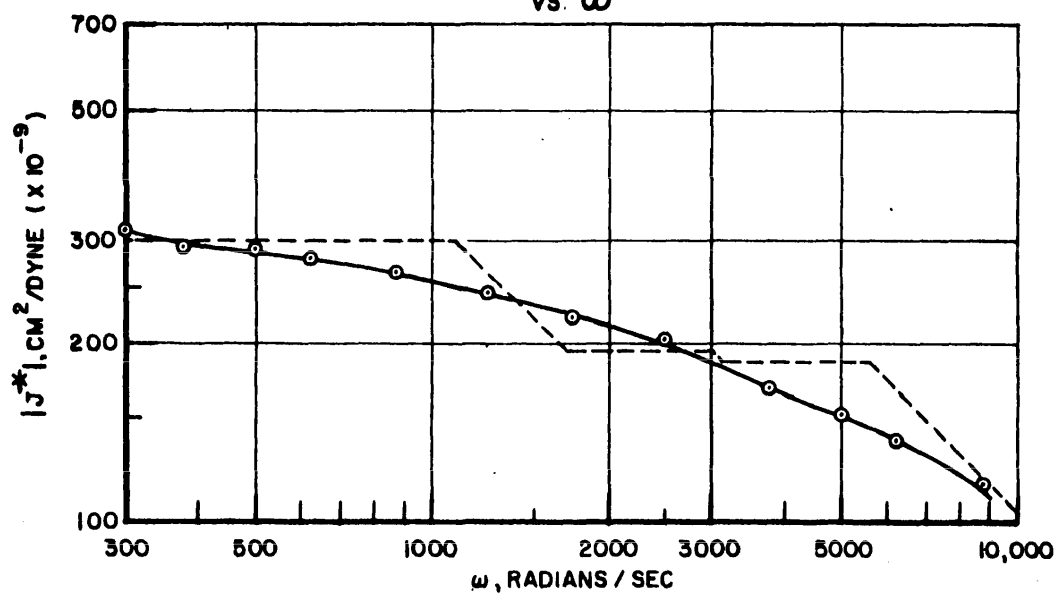
On the graphs of log J^* vs log ω are shown the straight-line approximations made by the method of asymptotic slopes,[8], [9] using the calculated poles and zeros. These straight-line approximations do not completely follow the calculated curve in some cases; this effect results from the interaction of errors. The approximation error at an isolated pair of critical values μ_i, λ_i is given by[8]

$$\log \frac{y(\lambda_i)}{\Gamma(\lambda_i)} = \log \frac{\Gamma(\mu_i)}{y(\mu_i)} = \log \sqrt{2} - \frac{1}{2} \log \left(1 + \frac{\lambda_i^2}{\mu_i^2}\right) \tag{24}$$

It a pair of critical values in which the ratio $\dfrac{\lambda_i}{\mu_i}$ is fairly large is followed by a pair in which it is relatively smaller, the two errors may interact. However, such fluctuations are of little importance, since in most cases a knowledge of the phase angle will permit the approximation to be made with sufficient accuracy for the use of the computer program mentioned previously. In 90% of the trials made in fitting the polyisobutylene data, the first choice of the λ_j provided a fair fit for the experimental data. These models generally were within $\pm 5\%$ in the middle range of data with some having errors of $\pm 10\%$ at the extremes. Slight adjustment of the λ_j resulted in models which fit the data at 92% of the data points with an accuracy of $\pm 5\%$ and with only one data point deviating by more than 10%.

Of significant importance is the fact that once the λ_j have been determined for a particular set of experimental data, introduction of new data which are more or less consistent with the old does not require selection of new λ_j, but only requires the use of the computer program to recalculate the other model parameters. As an example, recent data on polyisobutylene at $T = 25^\circ C$[13] which differ from the Fitzgerald data by approximately 10% were fitted using the same λ_j. Then by taking the geometric mean of the two sets of model constants, the model which best fits all the experimental data was determined and the resultant values of J' and J'' are displayed in Figures (19) and (20).

FIG. 10 - SHEAR COMPLIANCE J' FOR POLYISOBUTYLENE
AT INDICATED TEMPERATURES
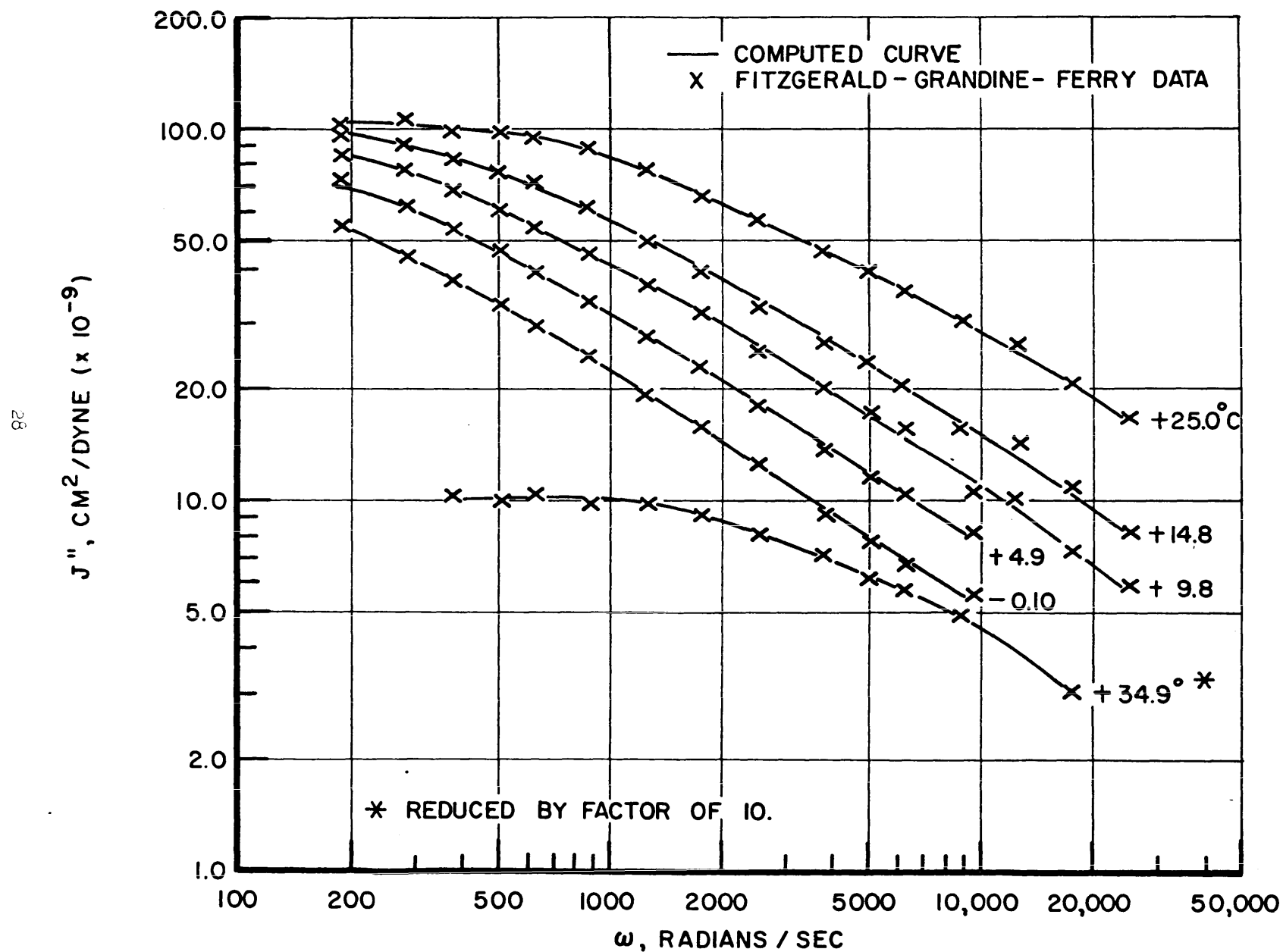### vs. ω
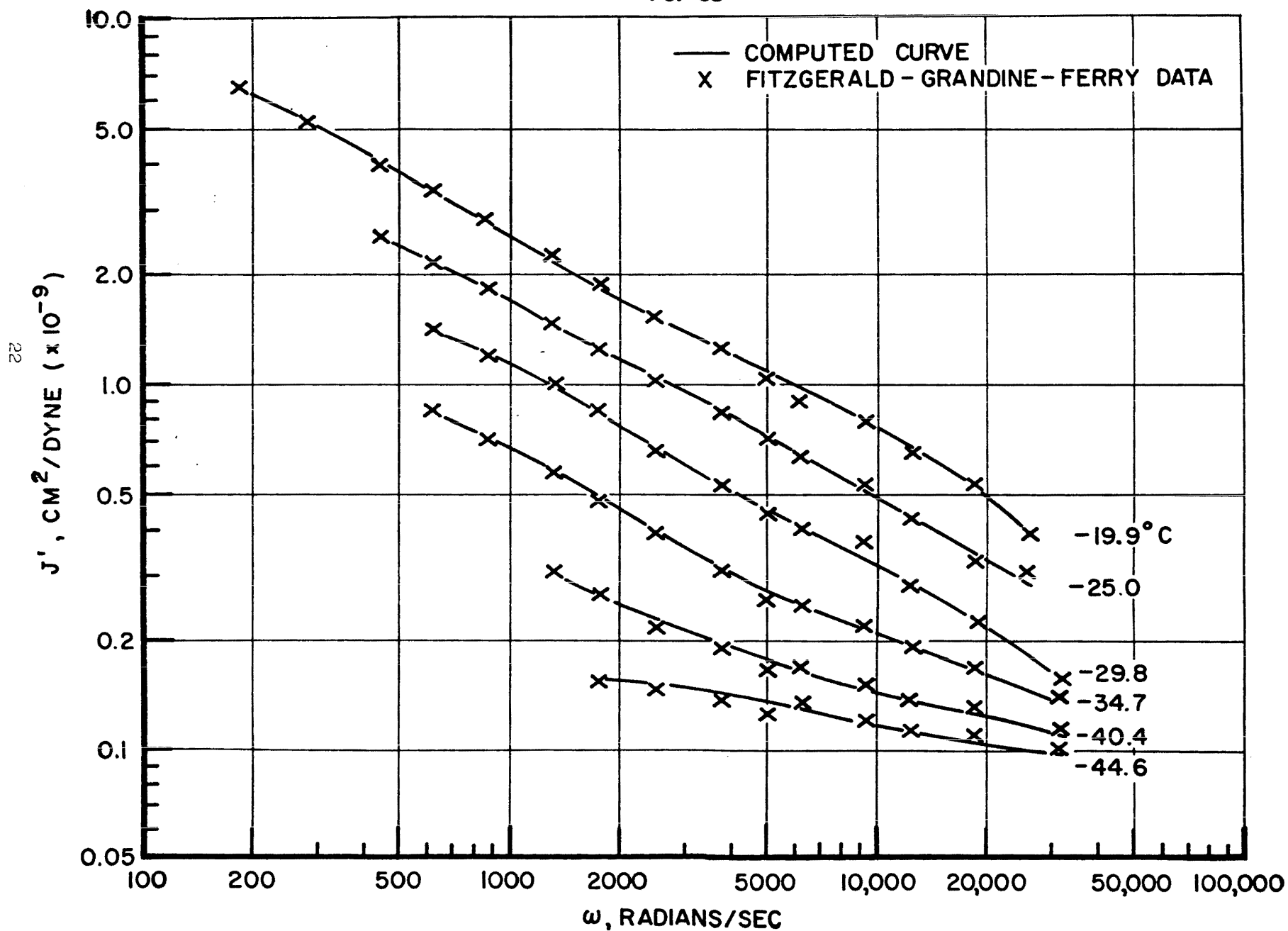
FIG. II - SHEAR COMPLIANCE J' FOR POLYISOBUTYLENE AT INDICATED TEMPERATURES vs. ω
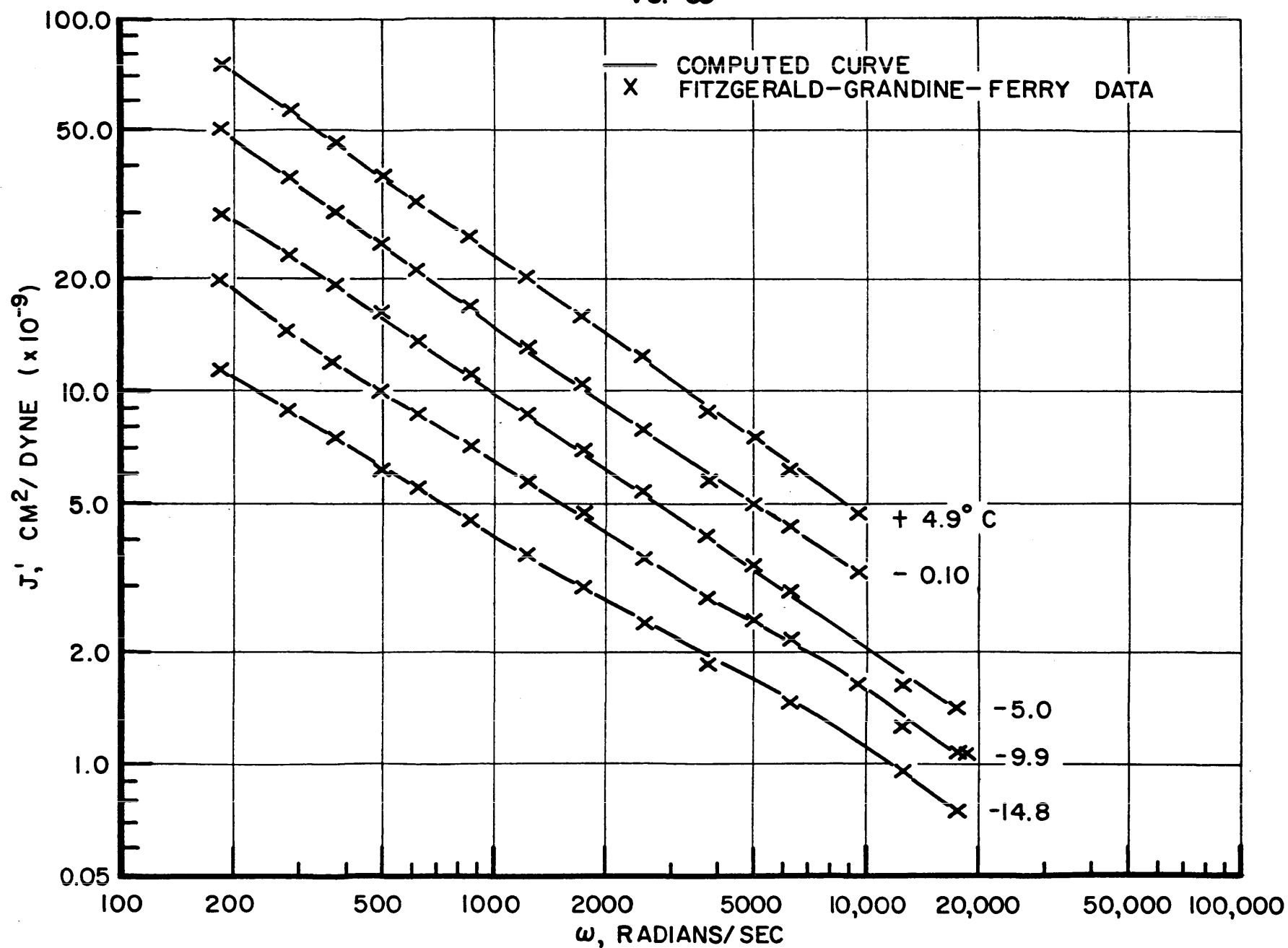
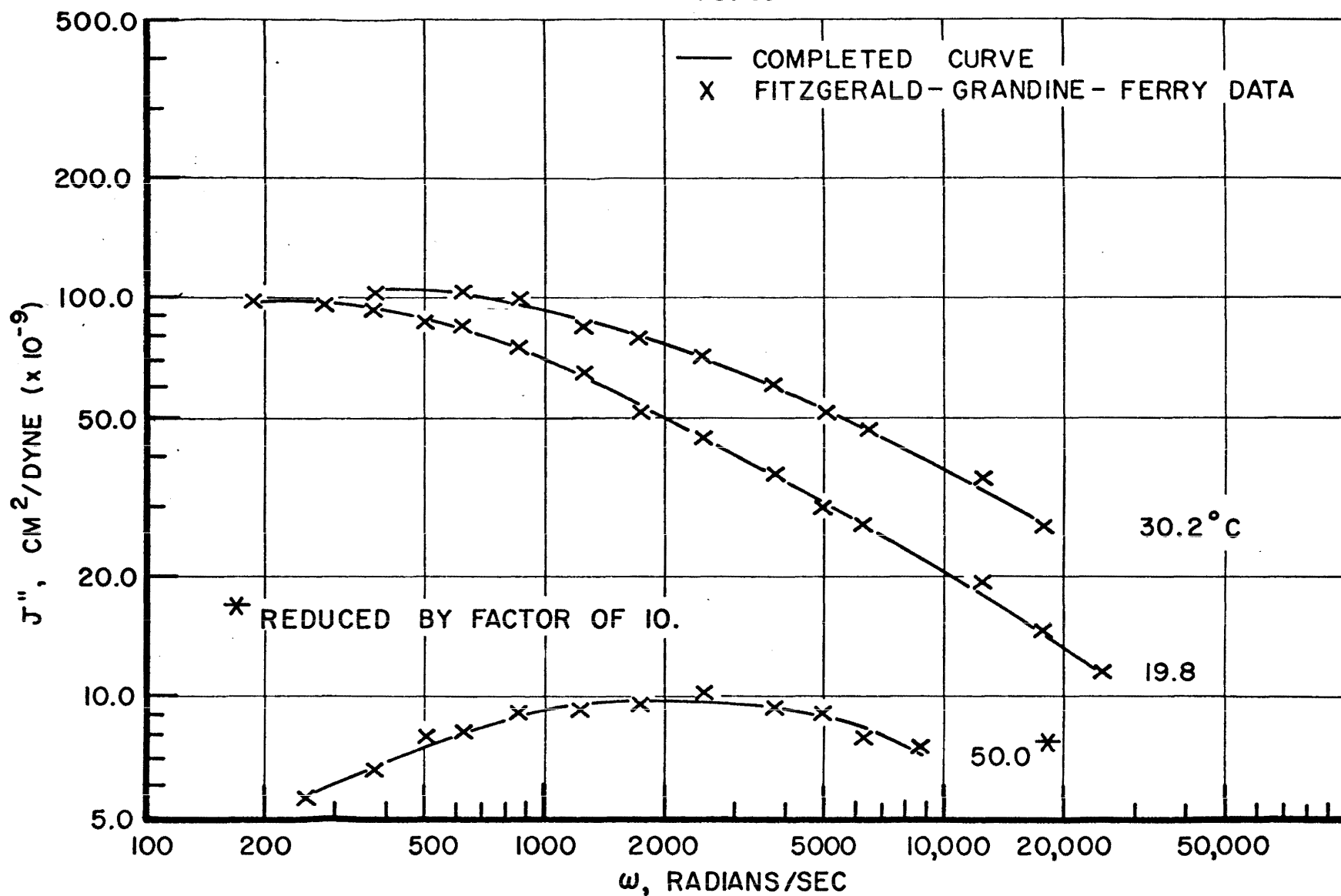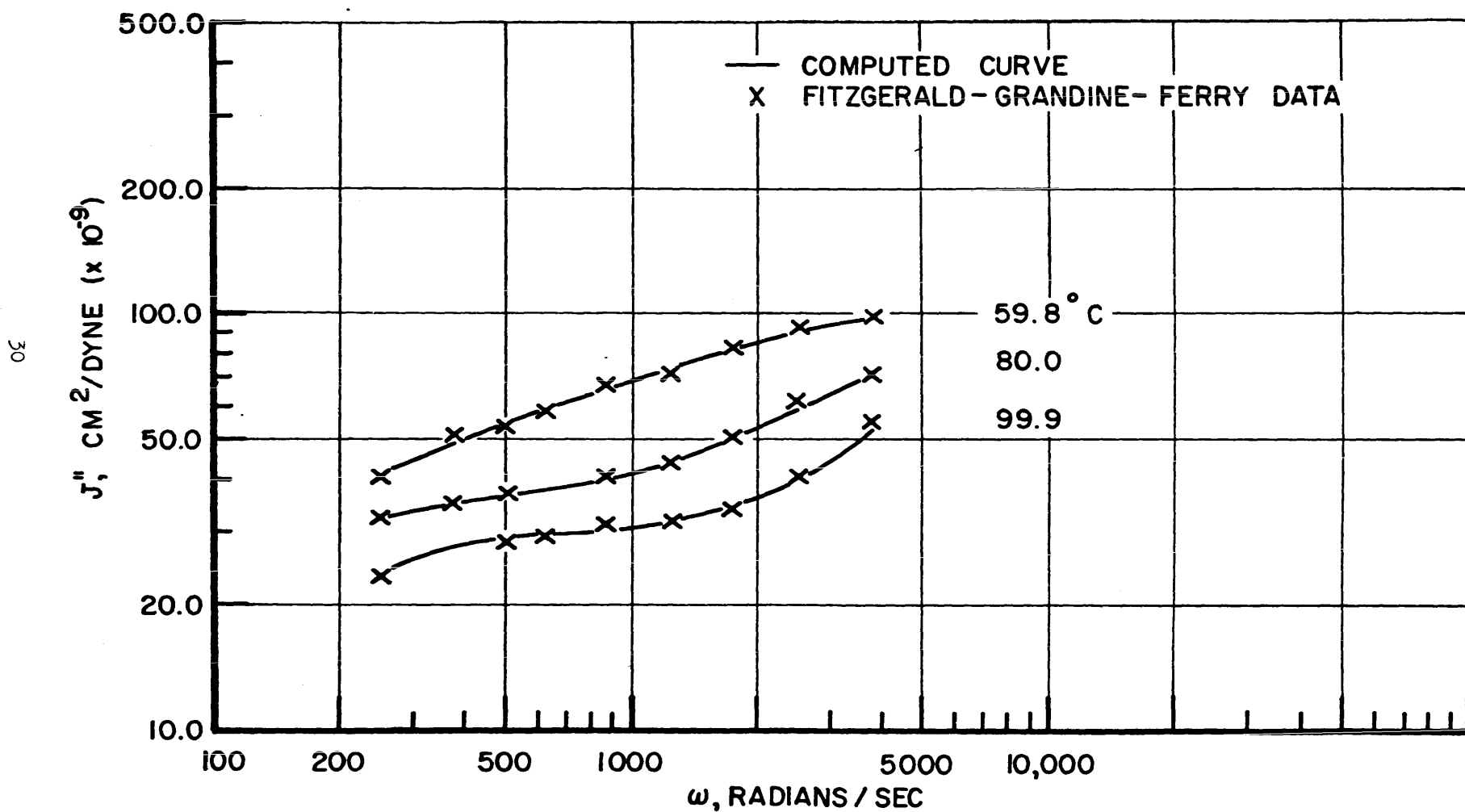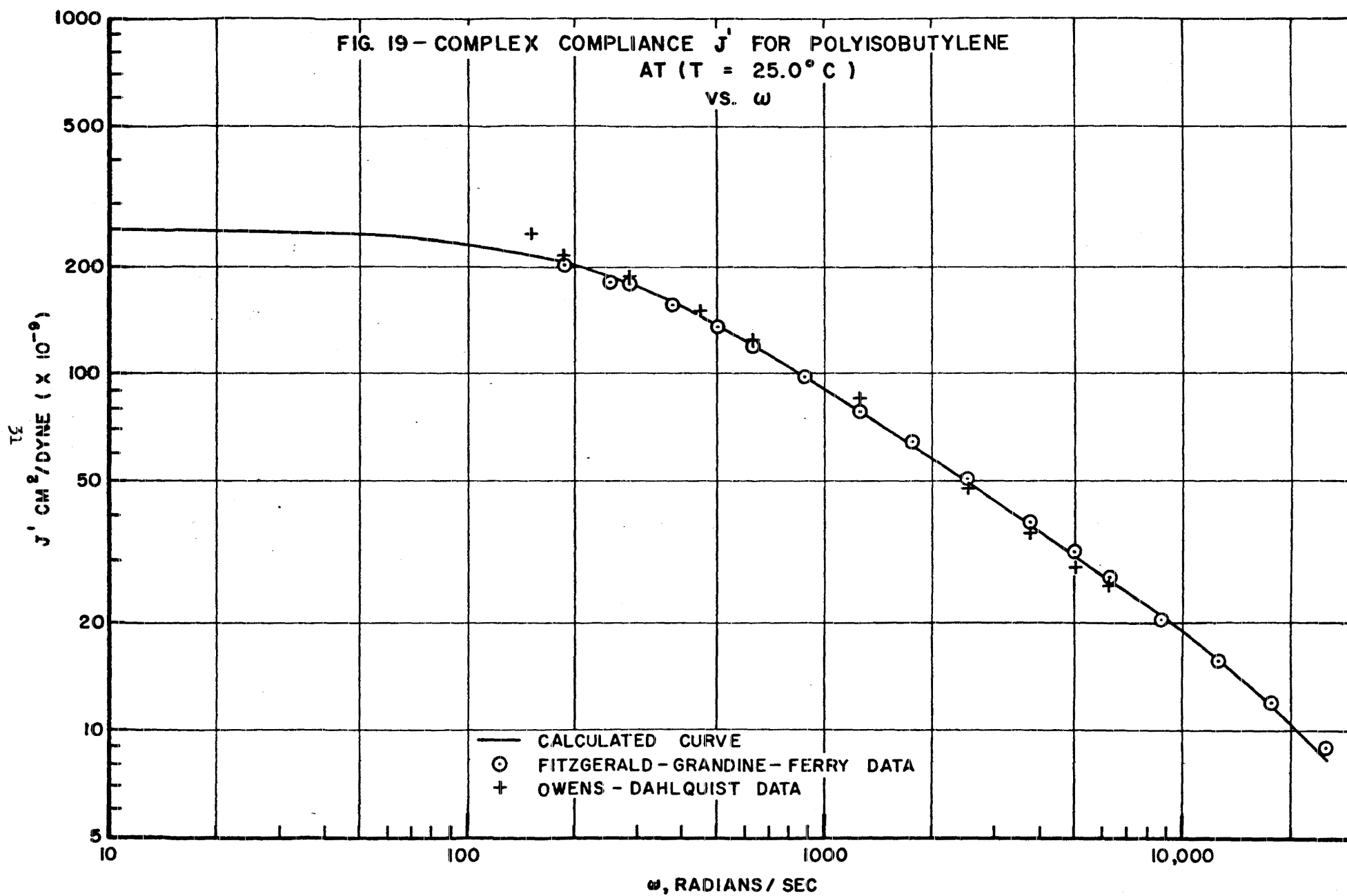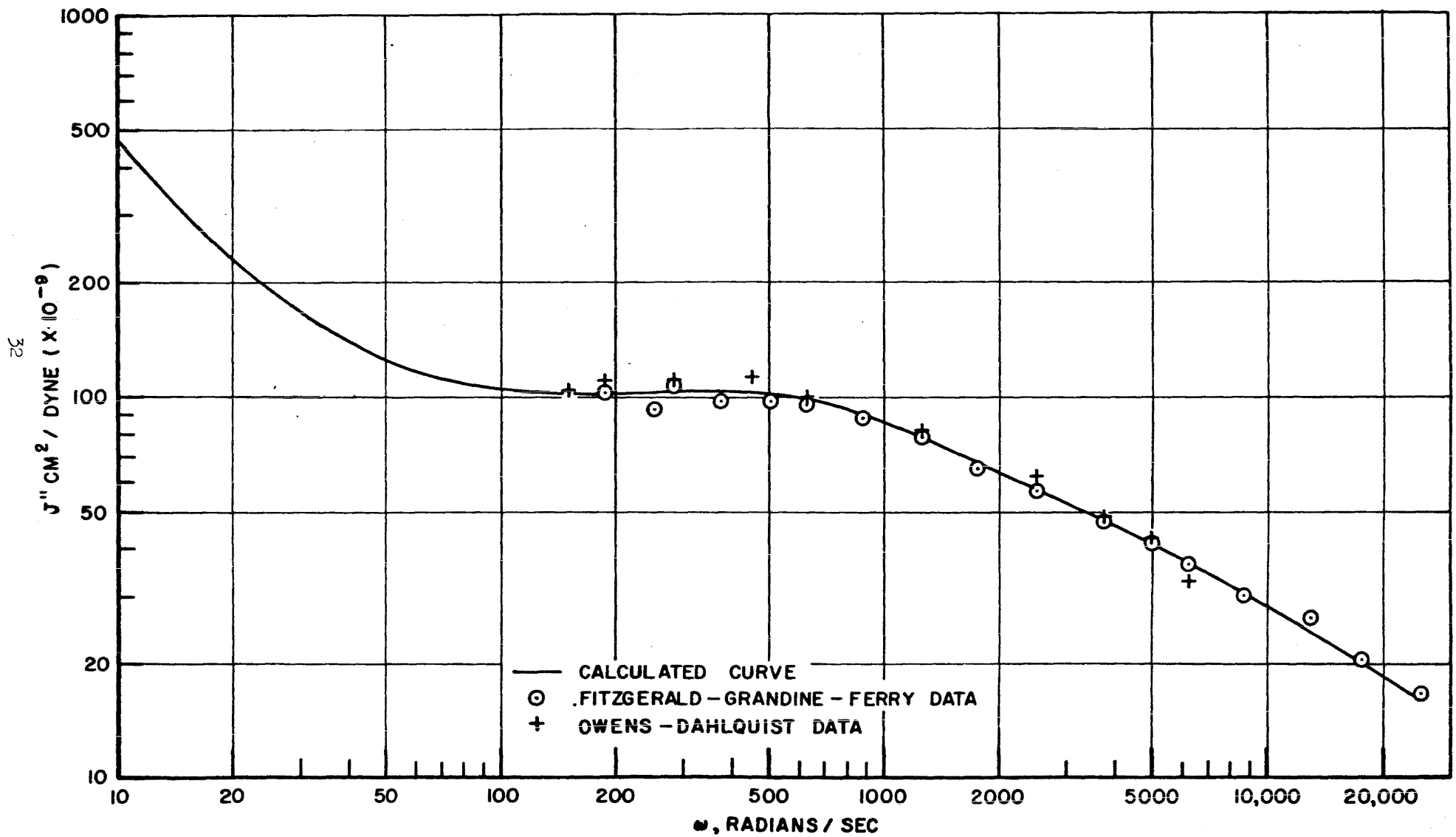FIG. 12 – SHEAR COMPLIANCE J' FOR POLYISOBUTYLENE AT INDICATED TEMPERATURES vs. ω

COMPUTED CURVE
X   FITZGERALD – GRANDINE – FERRY DATA

50.0° C

34.9

30.2

+ 25.0

+ 19.8

+ 14.8

+ 9.8

ω, RADIANS/SEC

100   200   500   1000   2000   5000   10,000   20,000   50,000   100,000

J', CM²/DYNE ($\times 10^{-9}$)

500.0   200.0   100.0   50.0   20.0   10.0   5.0   2.0
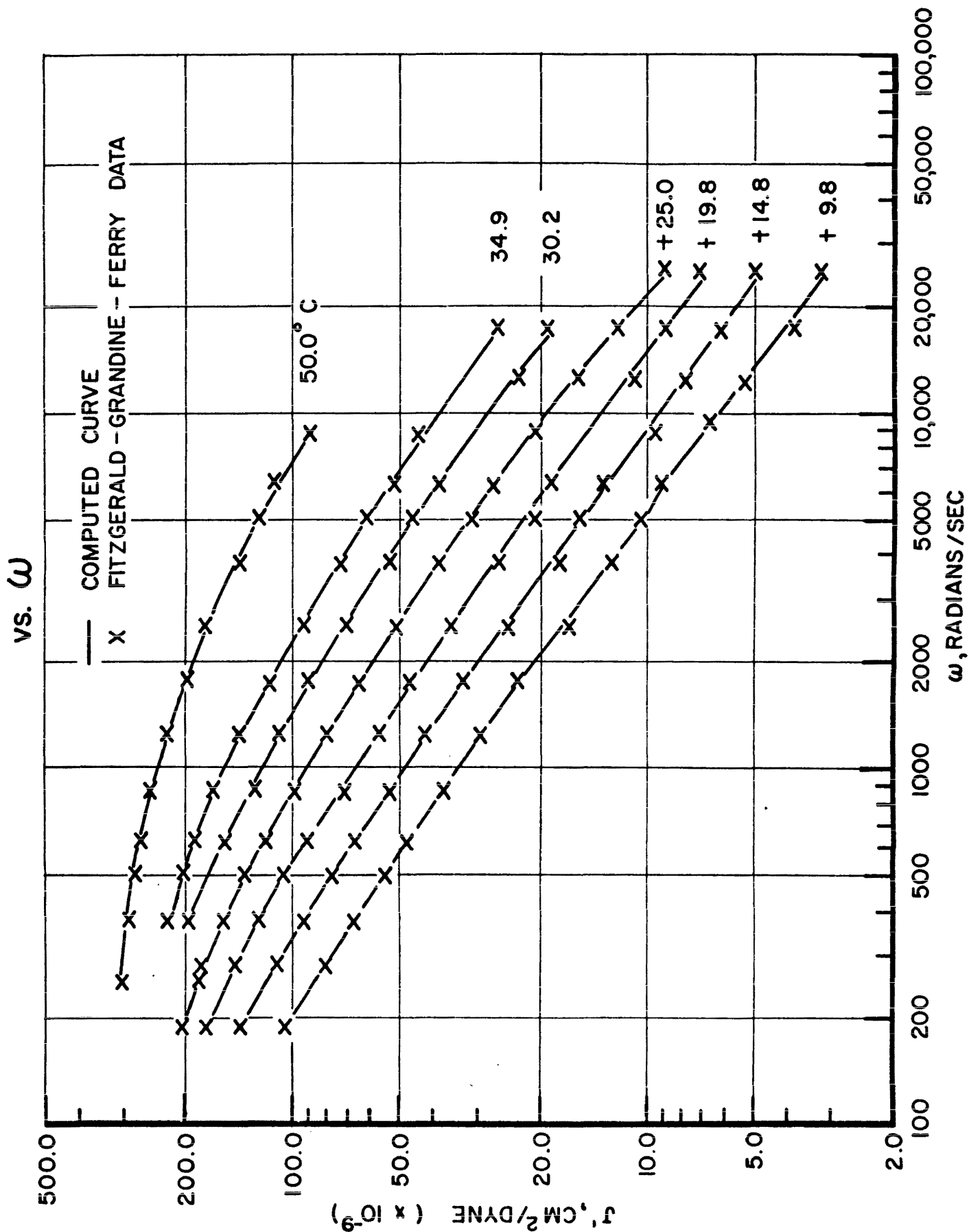
FIG. 13 — SHEAR COMPLIANCE J' FOR POLYISOBUTYLENE AT INDICATED TEMPERATURES vs. ω

FIG. 14 — SHEAR COMPLIANCE J" FOR POLYISOBUTYLENE AT INDICATED TEMPERATURES vs. ω
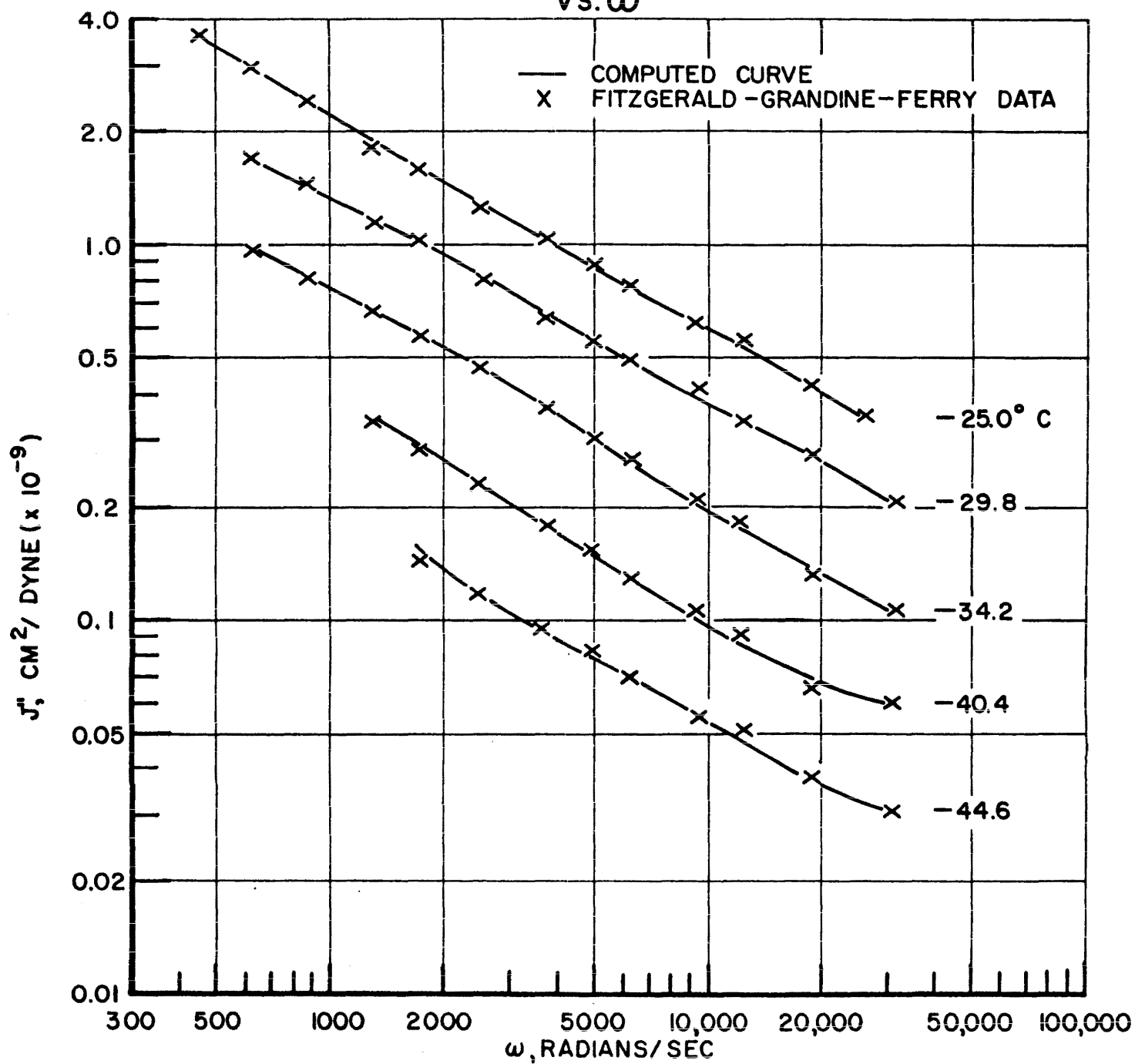
COMPUTED CURVE
X   FITZGERALD—GRANDINE—FERRY DATA

FIG. 15 – SHEAR COMPLIANCE J'' FOR POLYISOBUTYLENE AT INDICATED TEMPERATURES vs. ω

COMPUTED CURVE
X FITZGERALD – GRANDING – FERRY DATA

−5.0°C
−9.9
−14.8
−19.9
+40.0 *

* REDUCED BY FACTOR OF 100

ω, RADIANS/SEC

J'', CM²/DYNE (× 10⁻⁹)

27

FIG. 16 – SHEAR COMPLIANCE J" FOR POLYISOBUTYLENE
AT INDICATED TEMPERATURES
vs. ω

— COMPUTED CURVE
X FITZGERALD – GRANDINE – FERRY DATA

J", CM²/DYNE ($\times 10^{-9}$)

+25.0°C
+14.8
+4.9
+9.8
−0.10
+34.9° ✳

✳ REDUCED BY FACTOR OF 10.

ω, RADIANS / SEC
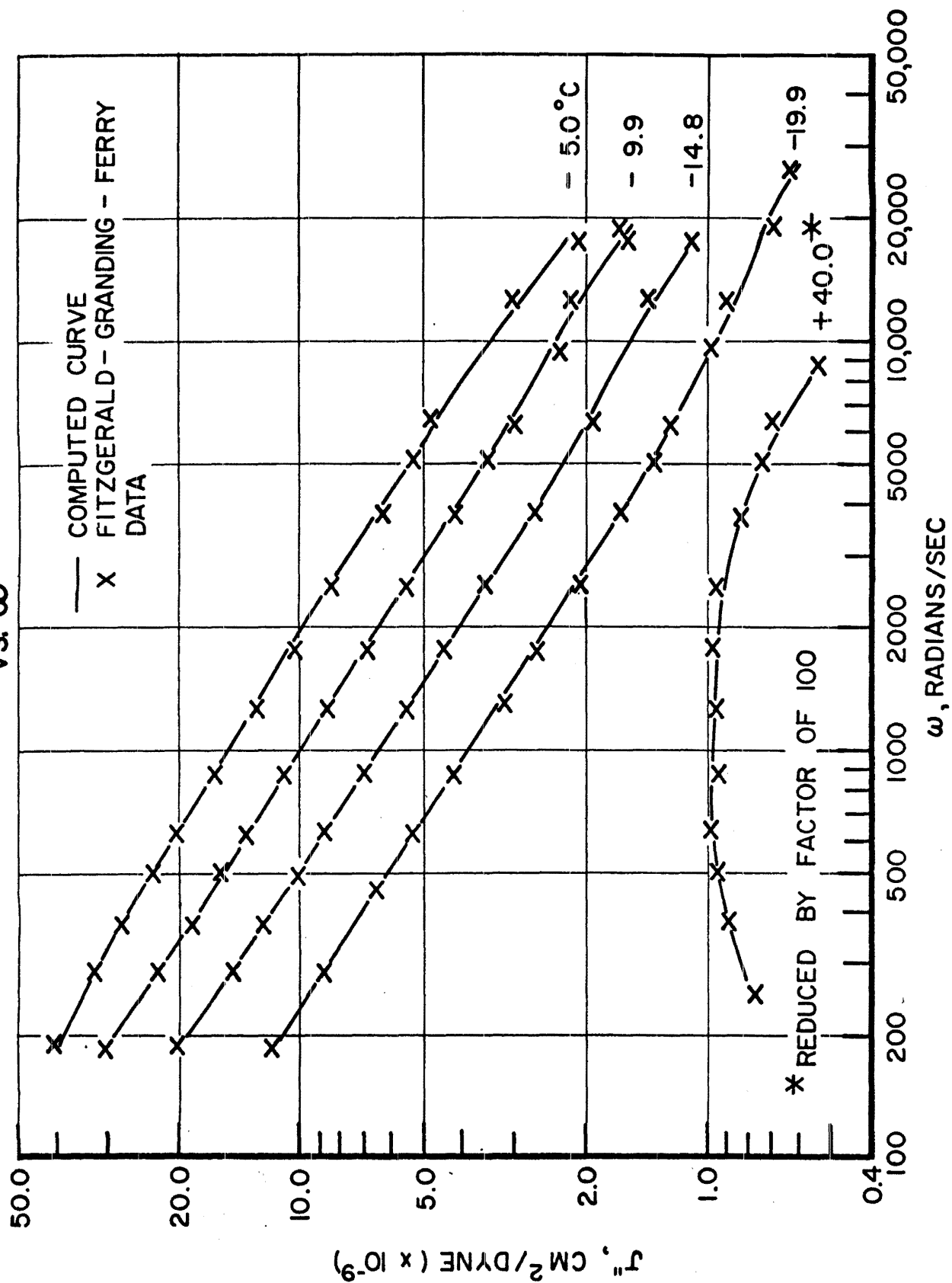
FIG. 17 – SHEAR COMPLIANCE J" FOR POLYISOBUTYLENE AT INDICATED TEMPERATURES vs. ω

FIG. 18 – SHEAR COMPLIANCE J" FOR POLYISOBUTYLENE AT INDICATED TEMPERATURES vs. ω

FIG. 19 – COMPLEX COMPLIANCE J' FOR POLYISOBUTYLENE AT (T = 25.0° C) VS. ω

CALCULATED CURVE
⊙ FITZGERALD – GRANDINE – FERRY DATA
+ OWENS – DAHLQUIST DATA

J' CM²/DYNE (X 10⁻⁹)

ω, RADIANS / SEC

FIG.20— COMPLEX COMPLIANCE J" FOR POLYISOBUTYLENE AT (T = 25.0° C) VS. ω

— CALCULATED CURVE
⊙ .FITZGERALD — GRANDINE — FERRY DATA
+ OWENS — DAHLQUIST DATA

ω, RADIANS / SEC

J" CM² / DYNE (X 10⁻⁶)

SUMMARY AND CONCLUSIONS
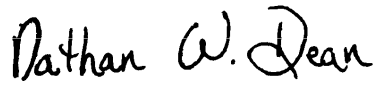
The results show that the combination of the semi-analytical and least squares computer program techniques readily produces models that fit experimental data over a 3 decade range of frequency. The models generated by this method can describe a wide range of viscoelastic behavior with a nominal accuracy of $\pm 5\%$. The application of this method, however, is limited to materials that behave in such a manner as to have $\left| J^*(\omega) \right|$ a monotonically decreasing function of ω whose slope is always greater than minus one when plotted on a log-log graph. If the material does not quite meet this criterion, as in polyisobutylene at $T = -44.6^\circ C$, $+80.0^\circ C$, and $+99.9^\circ C$, then the input data to the computer program must be adjusted to meet this requirement. Otherwise, the least squares program will yield negative C_j in attempting to fit the data. After making the necessary adjustments, the resultant model will still closely approximate the material behavior.

As more and more experimental data become available, the models generated by this method can easily be extended to fit a wider range of frequencies. Since these models describe the physical behavior of viscoelastic materials with an accuracy that is of the order of experimental errors, they can be used to formulate the stress-strain laws necessary to the solution of analytical problems. Laboratory experiments can then be conducted using the actual materials, and a comparison of analytical results with experimental results can then be made.

ACKNOWLEDGMENTS

The least squares procedure, and the program for zero determination were programmed by Mr. R. Abernathy under the supervision of Mr. G. Francis of the Computing Laboratory.

WILLIAM GOLDBERG
Capt, Ord Corps

NATHAN W. DEAN

REFERENCES

1. Lee, E. H. Viscoelastic Stress Analysis. Proc. 1st Symp. on Naval Structural Mechanics, Pergamon Press, Oxford: 456-482, 1960.

2. Bland, D. R. The Theory of Linear Viscoelasticity. New York: Pergamon Press, 1960.

3. Bland, D. R. and Lee, E. H. Jour. Appl. Mech., 23: 416, 1956.

4. Alfrey, T., Jr. Mechanical Behavior of High Polymers. New York Interscience Publishers, 1948.

5. Gross, B. Mathematical Structure of the Theories of Viscoelasticity. Paris: Herman and Cie., 1953.

6. Baum, R. F. A Contribution to the Approximation Problem. Proc. I.R.E., 36, No. 7: 863-869, July 1948.

7. Cauer, W., Die Verwirklichung von Wechselstromwiderstanden vorge-schriebener Frequenzabhangigkeit, Arch. Elektrotech., 17: 355-388, 1926.

8. Welch, J. T., Jr. Empirical Determination of Some Mathematical Models in Viscoelasticity. North Carolina State College, Contract No. DA-01-009-ORD-991: August 1961.

9. Chestnut, H. and Mayer, R. W. Servomechanisms and Regulating System Design, Vol I. New York: John Wiley & Sons, Inc., 1959.

10. Whittaker, E. and Robinson, G. The Calculus of Observations. London: Blackie and Son Ltd., 1944.

11. Elder, A. S. Calculation of Viscoelastic Model Constants from Complex Compliance Data. Bulletin of the Joint Meeting of the JANAF Panels on Physical Properties and Surveillance of Solid Propellants: 20-22 September 1960 (Confidential report).

12. Fitzgerald, E. R.; Grandine, L. D.; and Ferry, J. D. Dynamic Mechanical Properties of Polyisobutylene. Jour. of Appl. Phys., 24: 650-655, 1953.

13. Owens, K. E. and Dahlquist, C. A. Dynamic Mechanical Properties of Fluorochemical Elastomers. Trans. of the Soc. of Rheology, II: 23-37, 1958.

A P P E N D I C E S

A. SUMMARY OF SPRING-DASHPOT MODEL THEORY

B. EQUIVALENCE OF DIFFERENTIAL OPERATOR $\sigma - \epsilon$
    RELATION AND THE GENERALIZED VOIGT MODEL

Page intentionally blank

Page intentionally blank

Page intentionally blank

APPENDIX A

SUMMARY OF SPRING-DASHPOT MODEL THEORY

Combinations of spring and dashpot elements which form the spring-dashpot models, have been found to provide a convenient means for constructing a differential operator in order to approximate observed viscoelastic behavior. The basic elements of these models, as well as the two basic combinations of these elements are shown in Figure 1.
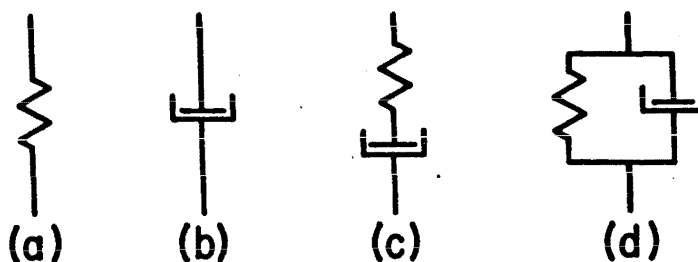
FIG. I. SIMPLE VISCOELASTIC ELEMENTS

The spring (Fig. 1.a) represents the elastic response of the material, and if σ and ϵ represent the stress and strain, then

$$\sigma(t) = E\epsilon(t) \tag{1}$$

where E is a constant called the modulus of the spring.

The dashpot, consisting of a piston, cylinder, and Newtonian fluid, represents the viscous flow of the material. The stress-strain relation is

$$\sigma(t) = \eta \frac{d\epsilon}{dt} \tag{2}$$

where η is a constant representing the viscosity of the fluid in the dashpot.

These two elements may be connected in two ways: (1) in series (Fig. 1.c) known as the Maxwell model, and (2) in parallel (Fig. 1.d) known as the Voigt or Kelvin model.

The stress-strain relation for the Maxwell model is

$$\frac{d\epsilon}{dt} = \frac{1}{E}\frac{d\sigma}{dt} + \frac{\sigma}{\eta} \tag{3}$$

and for the Voigt model is

$$\sigma(t) = E\epsilon(t) + \eta \frac{d\epsilon}{dt} \tag{4}$$

Comparison of the response of the Maxwell model and the Voigt model with actual materials has shown that models consisting of more elements are required to accurately describe the mechanical behavior of viscoelastic materials over a significant range of frequencies.

GENERALIZED MAXWELL MODEL

This model is an extension of the simple Maxwell model which can be used to describe a viscoelastic material.
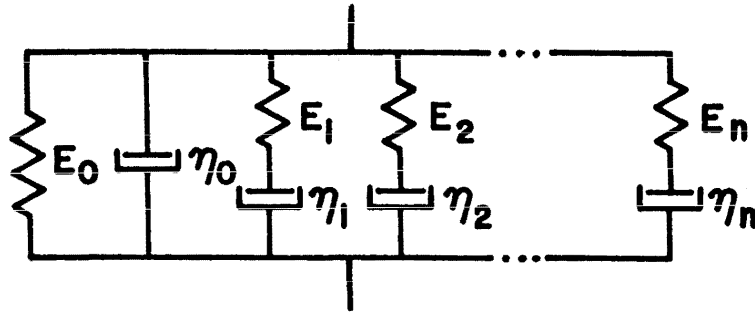
FIG. 2. THE GENERALIZED MAXWELL MODEL

The stress-strain relations derived from Figure 2 are given by

$$\epsilon = \epsilon_{E_0} = \epsilon_{\eta_0} = \epsilon_{E_i} + \epsilon_{\eta_i}$$

for $i = 1, 2, 3, \ldots n$

$$\sigma = \sigma_{E_0} + \sigma_{\eta_0} + \sigma_1 + \sigma_2 + \ldots + \sigma_n$$

$$\sigma_{E_0} = E_0 \epsilon$$

$$\sigma_{\eta_0} = \eta_0 \frac{d\epsilon}{dt} \tag{5}$$

$$\frac{d\epsilon}{dt} = \left[\frac{1}{E_1} \frac{d}{dt} + \frac{1}{\eta_1} \right] \sigma_1$$

$$\frac{d\epsilon}{dt} = \left[\frac{1}{E_2}\frac{d}{dt} + \frac{1}{\eta_2}\right]\sigma_2$$

$$\cdot \; \cdot \; \cdot \; \cdot \; \cdot \; \cdot \; \cdot \; \cdot \; \cdot \; \cdot \; \cdot$$

$$\frac{d\epsilon}{dt} = \left[\frac{1}{E_n}\frac{d}{dt} + \frac{1}{\eta_n}\right]\sigma_n$$

Combination of these equations yields the operational form:

$$\sigma(t) = \left[E_0 + \eta_0\left(\frac{d}{dt}\right) + \sum_{i=1}^{n} \frac{E_i\left(\frac{d}{dt}\right)}{\left(\frac{d}{dt} + \frac{E_i}{\eta_i}\right)}\right]\epsilon(t) \tag{6}$$

GENERALIZED VOIGT MODEL

This model is an extension of the simple Voigt model, and is the model used to describe the mechanical properties of the materials considered in this report. This model exhibits both instantaneous elasticity and long term
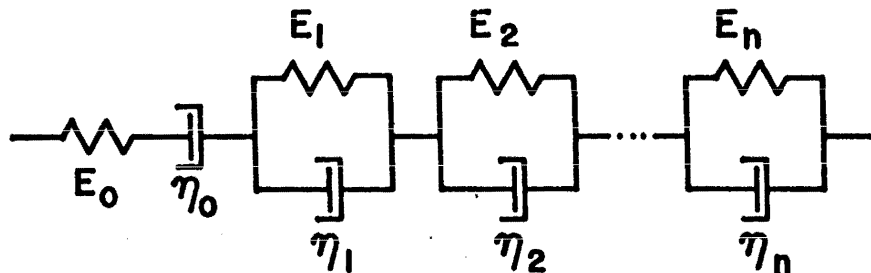
FIG. 3. THE GENERALIZED VOIGT MODEL

creep and is mathematically better suited to describe experimental dynamic creep data than is the generalized Maxwell model.

The stress-strain relations derived from Fig. 3 are given by:

$$\sigma = E_0\epsilon_{E_0}$$

$$\sigma = \eta_0 \frac{d\epsilon_{\eta_0}}{dt}$$

$$\sigma = \eta_1 \frac{d\epsilon_1}{dt} + E_1\epsilon_1 \tag{7}$$

$$\cdot \; \cdot \; \cdot \; \cdot \; \cdot \; \cdot \; \cdot \; \cdot$$

$$\sigma = E_n \epsilon_n + \eta_n \frac{d\epsilon_n}{dt}$$

$$\epsilon = \epsilon_{\epsilon_0} + \epsilon_{\eta_0} + \epsilon_1 + \epsilon_2 + \ldots + \epsilon_n$$

Combination of Eqs. (7) yields,

$$\epsilon(t) = \frac{\sigma(t)}{E_0} + \left[\frac{1}{\eta_0 \frac{d}{dt}} + \sum_{i=1}^{n} \frac{1}{E_i + \eta_i \frac{d}{dt}} \right] \sigma(t) \qquad (8)$$

APPENDIX B

EQUIVALENCE OF DIFFERENTIAL OPERATOR $\sigma - \epsilon$ RELATION AND THE GENERALIZED VOIGT MODEL

The use of the generalized Voigt model to approximate viscoelastic behavior is based upon the equivalence of the model's resultant differential operator with the relation

$$P\left[\sigma\right] = Q\left[\epsilon\right]. \tag{1}$$

The differential operator form, for the generalized Voigt model, as found in Appendix A, is given by

$$\epsilon(t) = \frac{\sigma(t)}{E_0} + \left[\frac{1}{\eta_0 \frac{d}{dt}} + \sum_{i=1}^{n} \frac{1}{E_i + \eta_i \frac{d}{dt}}\right] \sigma(t). \tag{2}$$

For the case of steady state sinusoidal stresses and strains, we have found that for the model

$$J^*(i\omega) = \frac{1}{E_0} + \frac{1}{\eta_0 i\omega} + \sum_{j=1}^{n} \frac{1}{E_j + i\omega\eta_j} . \tag{3}$$

Letting $j = i\omega$

$$J^*(s) = \frac{1}{E_0} + \frac{1}{\eta_0 s} + \sum_{j=1}^{n} \frac{1}{E_j + \eta_j s} . \tag{4}$$

We have also shown that for steady state sinusoidal stresses and strains, the differential operator, $\sigma - \epsilon$, viscoelastic relation yields

$$J^*(i\omega) = \frac{1 + p_1 i\omega + p_2 (i\omega)^2 + \ldots + p_m (i\omega)^m}{q_1 i\omega + q_2 (i\omega)^2 + \ldots + q_m (i\omega)^m} \tag{5}$$

Now let $i\omega = s$. Then

$$J^*(s) = H(s) = \frac{p(s)}{q(s)} = \frac{1 + p_1 s + p_2 s^2 + \ldots + p_m s^m}{q_1 s + q_s s^2 + \ldots + q_m s^m} \tag{6}$$

where $H(s)$ is defined as the system transfer function.

To show the equivalence of Eqs. (6) and (4), let $\lambda_1, \lambda_2, \lambda_3, \ldots \lambda_{m-1}$ be roots of the equation

$$q_1 + q_2 s + q_3 s^2 + \ldots + q_m s^{m-1} = 0 \tag{7}$$

The roots of this equation must be distinct, since we are considering only non-degenerate models. Then, the partial fraction expansion for $H(s)$ is given by:

$$H(s) = \frac{p_m}{q_m} + \frac{1}{q_1 s} + \sum_{j=1}^{m-1} \frac{1}{s - \lambda_j} \frac{p(\lambda_j)}{q'(\lambda_j)} \qquad (8)$$

Now let $m - 1 = n$, then

$$H(s) = \frac{p_m}{q_m} + \frac{1}{q_1 s} + \sum_{j=1}^{n} \frac{1}{s - \lambda_j} \frac{p(\lambda_j)}{q'(\lambda_j)} \qquad (9)$$

Comparison of Eqs. (9) and (4) yields

$$E_0 = \frac{q_m}{p_m} ; \quad \eta_0 = q_1 ; \quad \eta_j = \frac{q'(\lambda_j)}{p(\lambda_j)}$$

$$\qquad (10)$$

and

$$E_j = \frac{q'(\lambda_j)}{p(\lambda_j)} \lambda_j$$

which then yields

$$\lambda_j = - \frac{E_j}{\eta_j} . \qquad (11)$$

These equations relate the values of the model constants to the material constants in the stress-strain law. For a real mechanical system, E_j and η_j are real positive constants (or zero). Therefore, the λ_j are real and negative. This is a property of the transfer function, $H(s)$. As a direct result of the electrical network analogy,[4], [7], [8], [9] the following are the properties of the system transfer function, $H(s)$ for the generalized Voigt model:

(1) all zeros and poles of $H(s)$ occur on the negative axis of reals.

(2) all zeros and poles are simple, and are interlaced in the pattern... pole-zero-pole-zero-...

(3) the highest critical frequency of $H(s)$ is a zero; $H(\infty)$ is a positive real number.

(4) the lowest critical frequency of $H(s)$ is a pole which occurs at the origin, $s = 0$; $H(0) = \infty$.

DISTRIBUTION LIST

No. of Copies	Organization	No. of Copies	Organization

10	Commander
	Armed Services Technical
	    Information Agency
	ATTN: TIPCR
	Arlington Hall Station
	Arlington 12, Virginia
		1	Commanding General
			Ammunition Command
			ATTN: ORDLY-AREL, Engineering
			            Library
			Joliet, Illinois

1	Commanding General U. S. Army Materiel Command ATTN: AMCRD-RS-PE-Bal Research and Development Directorate Washington 25, D. C.	1	Commanding Officer U. S. Army Test Activity ATTN: ORDBG-TA-ET-AA Yuma Test Station, Arizona
1	Commanding General Frankford Arsenal ATTN: Propellant and Explosives Section 1331 Philadelphia 37, Pennsylvania	3	Commanding General White Sands Missile Range ATTN: ORDBS-OM-TL New Mexico
2	Commanding Officer Picatinny Arsenal ATTN: Library Dover, New Jersey	1	Commanding Officer Army Research Office (Durham) Box CM, Duke Station Durham, North Carolina

5	Redstone Scientific Information
	    Center
	ATTN: Chief, Document Section
	U. S. Army Missile Command
	Redstone Arsenal, Alabama
		3	Chief, Bureau of Naval Weapons
			ATTN: RMMP-2
			            RMMP-331
			            RRRE-6
			Department of the Navy
			Washington 25, D. C.

4	Commanding General
	U. S. Army Missile Command
	ATTN: Deputy Commanding
	            General for
	            Guided Missile -
	        Technical Library
	Redstone Arsenal, Alabama
		1	Commander
			Naval Missile Center
			ATTN: Technical Library
			Point Mugu, California

1	Commanding Officer Harry Diamond Laboratories ATTN: Technical Information Office Branch 012 Washington 25, D. C.	2	Commander U. S. Naval Ordnance Laboratory ATTN: Library White Oak Silver Spring, Maryland
		2	Commander U. S. Naval Ordnance Test Station ATTN: Technical Library Branch China Lake, California

DISTRIBUTION LIST

No. of Copies	Organization	No. of Copies	Organization
2	Commanding Officer U. S. Naval Propellant Plant ATTN: Technical Library Indian Head, Maryland	7	Director National Aeronautics and Space Administration ATTN: Office of Technical Information and Educational Programs, Code ETL 1520 H. Street, N. W. Washington 25, D. C.
1	Commander U. S. Naval Weapons Laboratory ATTN: Technical Library Dahlgren, Virginia		
1	Commanding Officer Office of Naval Research 1030 E. Green Street Pasadena 1, California	1	Aerojet-General Corporation ATTN: Florence Walsh, Librarian 11711 South Woodruff Avenue Downey, California
1	Director Special Projects Office Department of the Navy Washington 25, D. C.	2	Aerojet-General Corporation ATTN: Librarian P.O. Box 296 Azusa, California
1	Commander Space Systems Division Air Force Systems Command ATTN: TDC P. O. Box 262 Air Force Unit Post Office Los Angeles 45, California	3	Aerojet-General Corporation ATTN: Technical Information Office P.O. Box 1947 Sacramento, California
		2	Aerospace Corporation ATTN: Library Documents P.O. Box 95085 Los Angeles 45, California
1	Commander Rocket Research Laboratories Air Force Systems Command ATTN: DGS Edwards, California	1	Allied Chemical Corporation General Chemical Division Research Laboratory ATTN: L. J. Wiltrakis - Security Office P.O. Box 405 Morristown, New Jersey
1	Commander Air Proving Ground Center ATTN: PGAPI Eglin Air Force Base, Florida	1	American Cyanamid Company ATTN: Dr. A. L. Peiker 1937 W. Main Street Stamford, Connecticut
2	U.S. Department of the Interior of Mines ATTN: M. M. Dolinar, Reports Librarian Explosives Research Laboratory 4800 Forbes Street Pittsburgh 13, Pennsylvania	1	Aeronautical Systems Division Wright-Patterson Air Force Base, Ohio ATTN: ASRCEM-1

DISTRIBUTION LIST

No. of Copies	Organization	No. of Copies	Organization
1	American Machine and Foundry Company Mechanics Research Department ATTN: Phil Rosenberg 7501 North Natchez Avenue Niles 48, Illinois	1	The Franklin Institute ATTN: Miss Marion H. Johnson, Librarian Technical Reports Library 20th and Parkway Philadelphia 3, Pennsylvania
1	Armour Research Foundation Illinois Institute of Technology Technology Center ATTN: Fluid Dynamics and Propulsion Research, Department D Chicago 16, Illinois	1	Hercules Powder Company Allegany Ballistics Laboratory ATTN: Library P.O. Box 210 Cumberland, Maryland
1	Arthur D. Little, Inc. ATTN: W. H. Varley 15 Acorn Park Cambridge 40, Massachusetts	1	Hercules Powder Company ATTN: Technical Information Division Research Center (Dr. Herman Skolnik) 910 Market Street Wilmington 99, Delaware
2	Atlantic Research Corporation Shirley Highway and Edsall Road Alexandria, Virginia	1	Hercules Powder Company Bacchus Works ATTN: Librarian Magna, Utah
1	Callery Chemical Company Research and Development ATTN: Document Control Callery, Pennsylvania	1	The Martin Company ATTN: Library Orlando, Florida
1	The Dow Chemical Company ATTN: Dr. R. S. Karpink 1710 Building Security Section, Box 31 Midland, Michigan	1	The Martin Company ATTN: T. W. Woodard Baltimore 3, Maryland
1	Esso Research and Engineering Company Chemicals Research Division ATTN: Dr. J. P. Longwell P.O. Box 51 Linden, New Jersey	1	Midwest Research Institute ATTN: Librarian 425 Volker Boulevard Kansas City 10, Missouri
		1	Minnesota Mining and Manufacturing Company ATTN: J. D. Ross 900 Bush Avenue St. Paul 6, Minnesota

DISTRIBUTION LIST

No. of Copies	Organization	No. of Copies	Organization
1	Forrestal Research Center Princeton University ATTN: Librarian Princeton, New Jersey	3	Olin Mathieson Chemical Corporation Research Library 1-K-3 ATTN: Mail Control Room - Miss Laura M. Kajuti 275 Winchester Avenue New Haven, Connecticut
1	Olin Mathieson Chemical Corporation ATTN: Research Library Box 508 Marion, Illinois	1	Thiokol Chemical Corporation Rocket Operations Center ATTN: Librarian P.O. Box 1640 Ogden, Utah
1	Pennsalt Chemicals Corporation ATTN: Dr. G. Barth-Wehrenalp Box 4388 Philadelphia 18, Pennsylvania	1	Thiokol Chemical Corporation Elkton Division ATTN: Librarian Elkton, Maryland
3	Rocketdyne ATTN: Library, Dept. 596-306 6633 Canoga Avenue Canoga Park, California	2	Thiokol Chemical Corporation Wasatch Division ATTN: Library Section P.O. Box 524 Brigham City, Utah
1	Rocketdyne, A Division of North American Aviation, Inc. Solid Propulsion Operations ATTN: Library P.O. Box 548 McGregor, Texas	1	Union Carbide Corporation ATTN: B. J. Miller 270 Park Avenue New York 17, New York
1	Rohm and Haas Company Redstone Arsenal Research Division ATTN: Librarian Huntsville, Alabama	1	United Technology Corporation ATTN: Librarian P.O. Box 358 Sunnyvale, California
1	Space Technology Laboratory, Inc. ATTN: Mr. Robert C. Anderson 5730 Arbor-Vitae Street Los Angeles 45, California	2	Wright Aeronautical Division Curtiss-Wright Corporation Wood-Ridge, New Jersey
2	Thiokol Chemical Corporation Redstone Division ATTN: Technical Director Huntsville, Alabama	1	California Institute of Technology Guggenheim Aeronautical Laboratory ATTN: Dr. M. L. Williams 1201 East California Street Pasadena 4, California

DISTRIBUTION LIST

No. of Copies	Organization	No. of Copies	Organization
1	Jet Propulsion Laboratory ATTN: I. E. Newlan, Chief, Reports Group 4800 Oak Grove Drive Pasadena 3, California	3	Solid Propellant Information Agency Applied Physics Laboratory The Johns Hopkins University Silver Spring, Maryland
1	Dr. J. H. Baltrukonis Catholic University of America Washington, D. C.	1	Dr. W. A. Nash University of Florida Gainsville, Florida
1	Columbia University Department of Civil Engineering and Engineering Mechanics ATTN: Dr. A. M. Freudenthal New York, New York	1	Dr. H. H. Hilton University of Illinois Urbana, Illinois
1	Mr. J. E. Fitzgerald Grand Central Rocket Co. Redlands, California	2	Mr. Nathan W. Dean c/o Physics Department University of North Carolina Chapel Hill, North Carolina
2	North Carolina State College Department of Mathematics ATTN: Dr. J. W. Cell Raleigh, North Carolina	1	Physics Department University of North Carolina Chapel Hill, North Carolina
1	Dr. J. M. Klosner Polytechnic Institute of Brooklyn Brooklyn, New York	10	Defence Research Staff British Embassy ATTN: The Scientific Information Officer 3100 Massachusetts Avenue, N. W. Washington 8, D. C.
1	Purdue University Department of Chemistry ATTN: Dr. Henry Feuer Lafayette, Indiana	4	Defence Research Member Canadian Joint Staff (W) 2450 Massachusetts Avenue, N.W. Washington 8, D. C.
1	Mr. C. H. Parr Rohm and Haas Company Huntsville, Alabama		
1	Southwest Research Institute Department of Structural Research ATTN: Dr. Robert C. DeHart, Director 8500 Culebra Road San Antonio 6, Texas		

AD   Accession No.   UNCIASSIFIED

Ballistic Research Laboratories, APG
DETERMINATION OF VISCOELASTIC MODEL CONSTANTS FROM
DYNAMIC MECHANICAL PROPERTIES OF LINEAR
VISCOELASTIC MATERIALS
W. Goldberg and N. W. Dean

	Elasticity -
	Mathematical analysis
	Viscoelastic materials
	Propellants -
	Mechanical properties

BRL Report No. 1180 November 1962

DA Project No. 517-06-002
UNCLASSIFIED Report

A semi-analytical method of determining the generalized Voigt model which represents the dynamic mechanical properties of a linear viscoelastic material over a range of frequencies of three decades is presented. This model representation is shown to be equivalent to the differential operator formulation of the linear viscoelastic stress-strain law. The method is applied to complex creep compliance data for N.B.S. polyisobutylene at 22 different temperatures. In general, the compliances calculated from the models differ from the experimental data by less than 5%.

A summary of spring-dashpot model theory is presented in Appendix A. The equivalence of the differential operator stress-strain relation and the generalized Voigt model is demonstrated in Appendix B.